Twenty Years of Experimental and DNS Access to the Velocity Gradient Tensor: What Have We Learned About Turbulence?

James M. Wallace

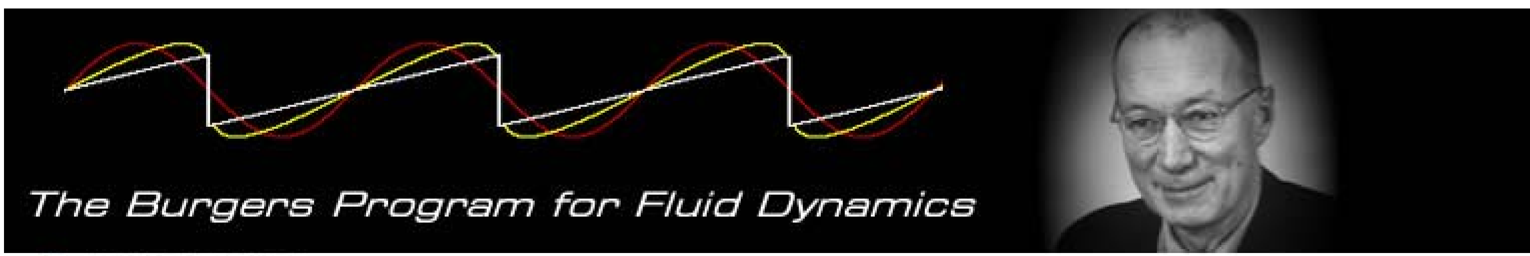

UNIVERSITY OF MARYLAND

Background & Overview

"…vorticity measurements suggest themselves as the most promising method for a quantitative study of ordered motion. …unfortunately…direct measurment of vorticity has not yet been sucessfully accomplished with sufficient accuracy." (Laufer, Ann. Rev. Fl. Mech. 7, 1975).

As recently as twenty years ago there was still no experimental or computational access to the velocity gradient tensor for turbulent flows. Vorticity, dissipation and strain rates and helicity, were inaccessible.

In 1987 measurements of all the components of the velocity gradient tensor in a turbulent boundary layer by a multi-sensor hot-wire probe were published *(Balint, Vukoslavčević & Wallace, Advances in Turbulence, Proc. 1st Euro. Turb. Conf.)*

In 1987 the first DNS of homogeneous turbulent shear flow *(Rogers & Moin, JFM 176 and* Ashurt, Kerstein, Kerr & Gibson and, Phys. Fluids 30*)* and of a turbulent channel flow *(Kim, Moin & Moser, JFM 177)* were successfully completed and reported.

PIV with sufficient spatial resolution was developed in the 1990's to provide another means of access to these fundamental properties of turbulence.

This presentation will review these remarkable developments and point out some of the most important things we have learned about turbulence as a result.

Acknowledgements

Co-workers:
Elias Balaras
Jean-Louis Balint
Peter Bernard
Lawrence Ong
Ugo Piomelli
Serge Simöens
Petar Vukoslavčević

Students:
Alan Folz
Eleftaris Kastrinakis
Rick Loucks
Ning Li
Seong-Ryong Park
Phuc Nguyen
Bill Wassmann

Colleagues:
Yannis Andreopoulos
Ron Adrian
Bob Brodkey
Jim Duncan
Helmut Eckelmann
John Foss
Fazle Hussain
Ken Kiger
John Kim
Parviz Moin
Bob Moser
Ron Panton
Mike Rogers
Phillipe Spalart
Arkady Tsinober …..

Support over the years by:
NSF, DOE, NASA, CTR summer program

Nine-Sensor Hot-wire Probe

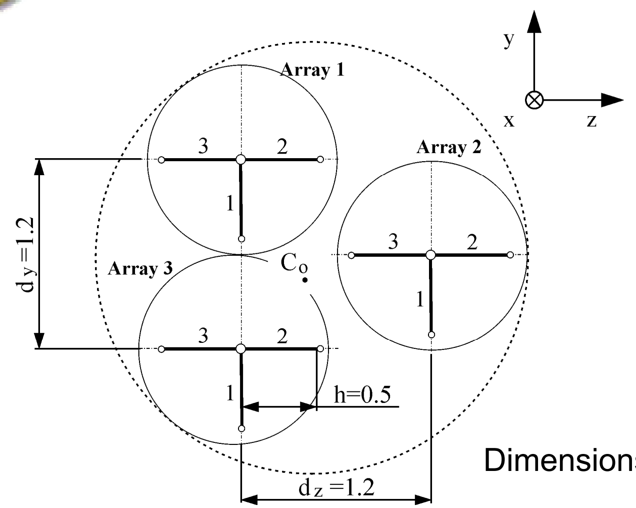

Dimensions in mm.

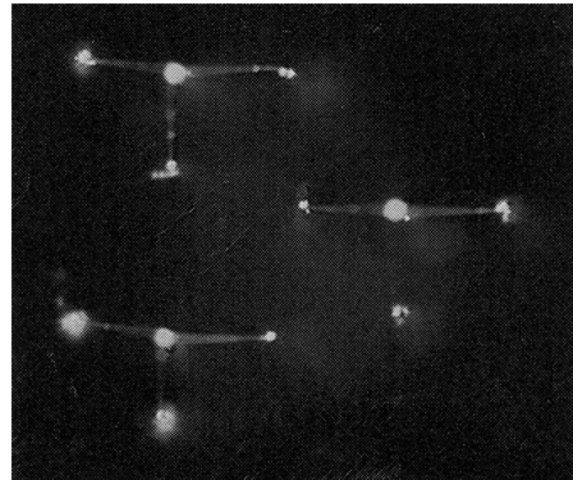

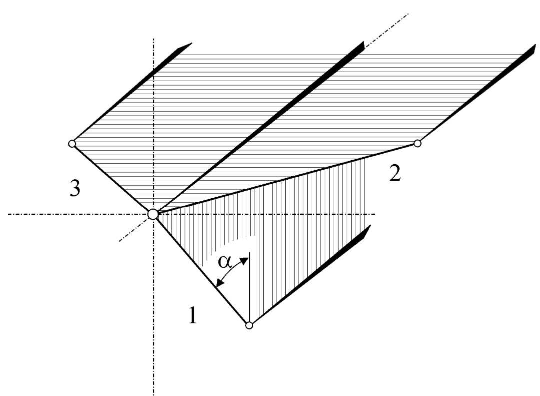

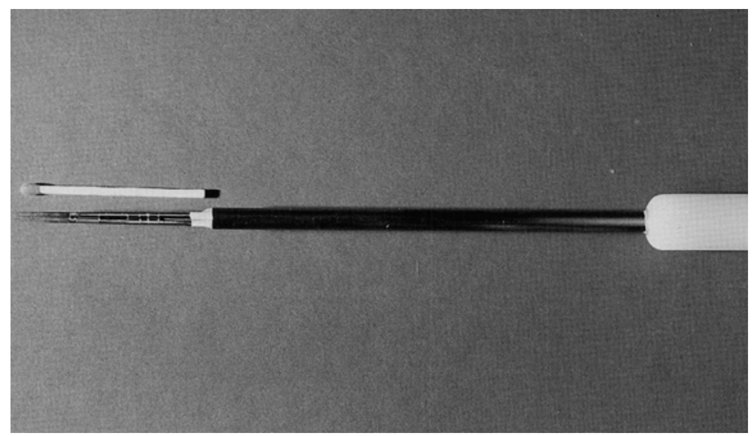

Vukoslavčević, Balint & Wallace. (1991)

JFM 228

Turbulent Kinetic Energy Production & Dissipation Rate in a Turbulent Boundary Layer

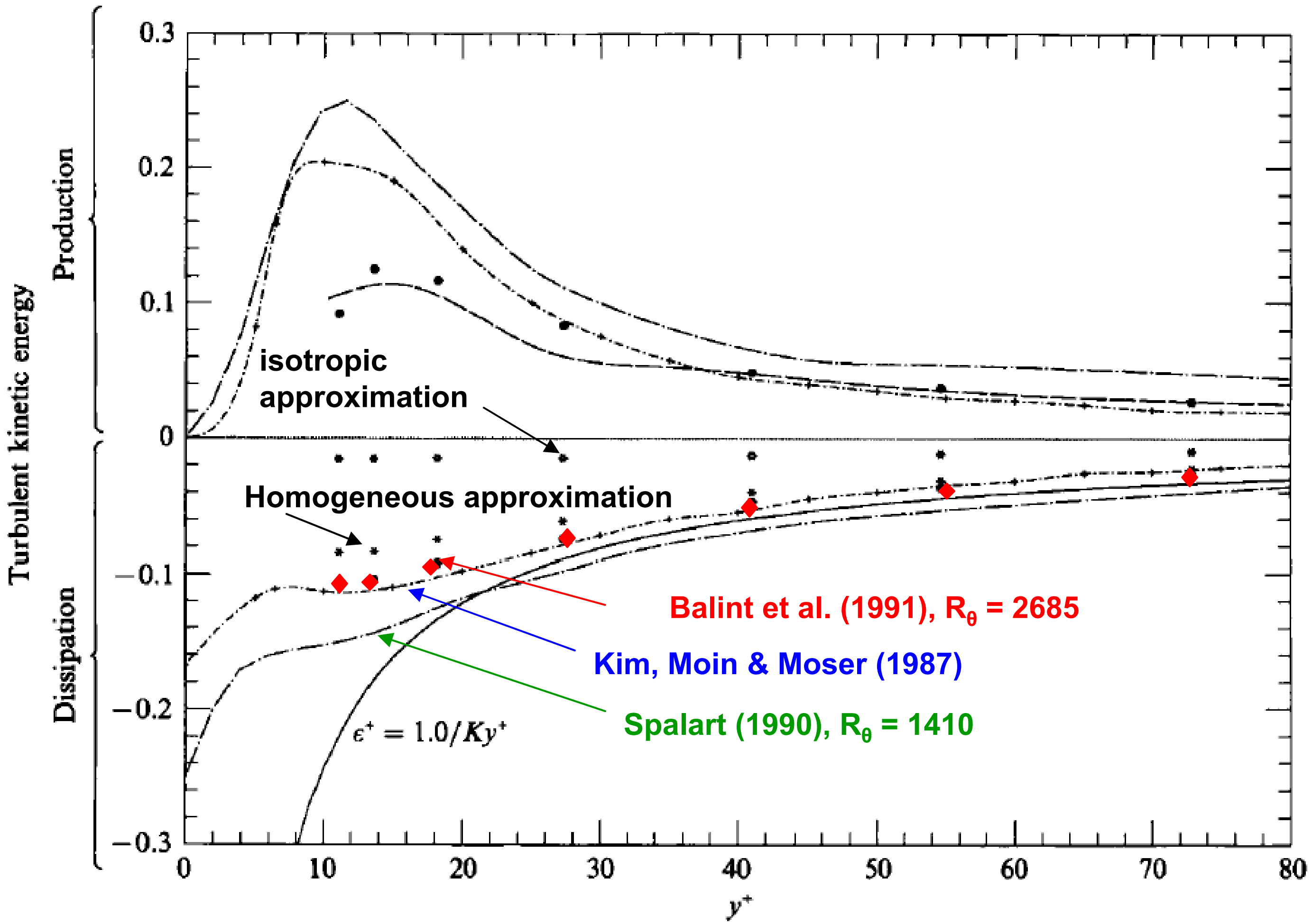

Balint, Vukoslavčević & Wallace. (1991)

JFM 228

DNS Turbulent Kinetic Energy Budget in a Supersonic Boundary Layer at Mach 2.5

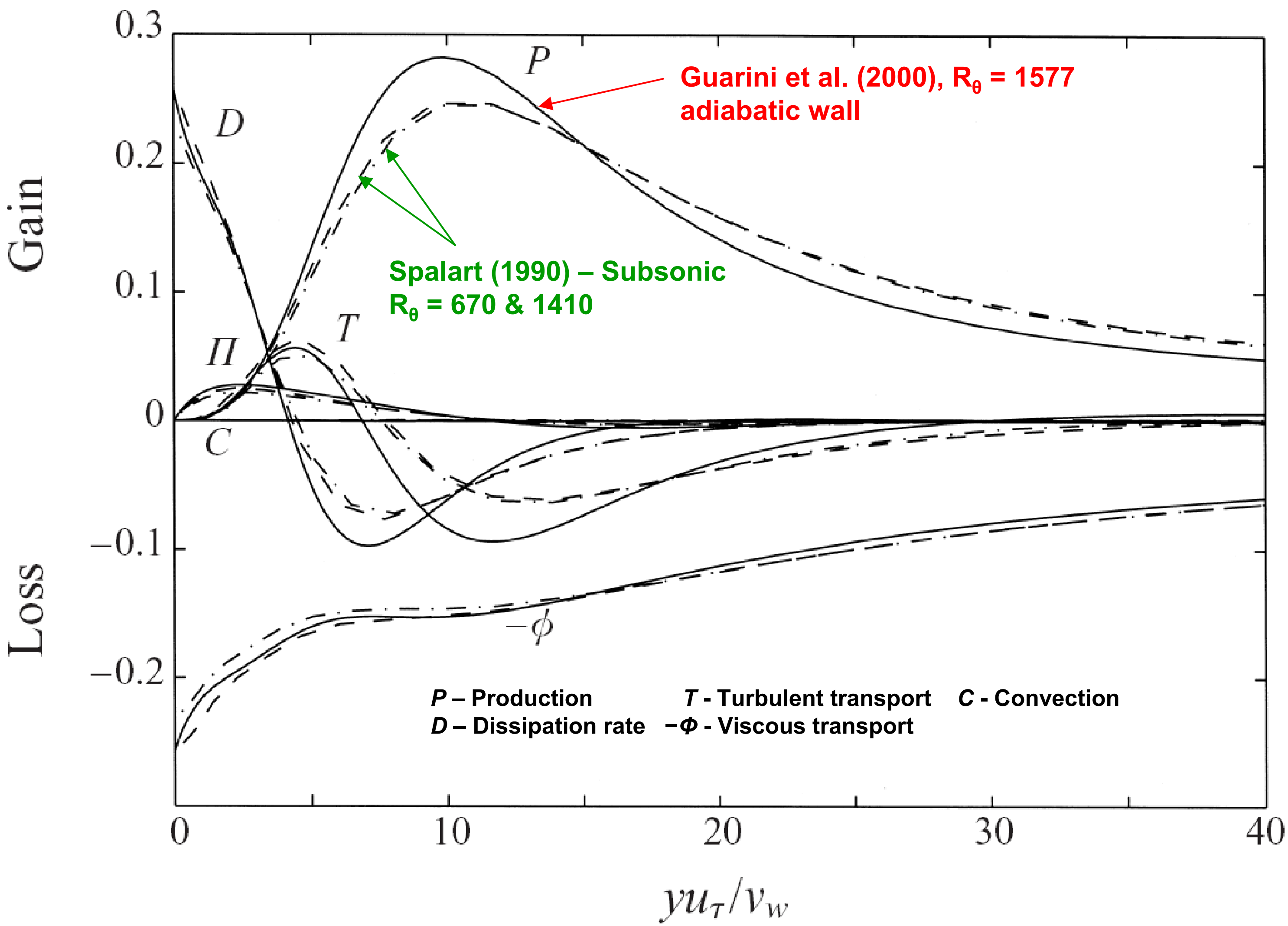

S. E. Guarini, R. D. Moser, K. Shariff & A. Wray (2000)

JFM 414

12-Sensor Hot-Wire Probe

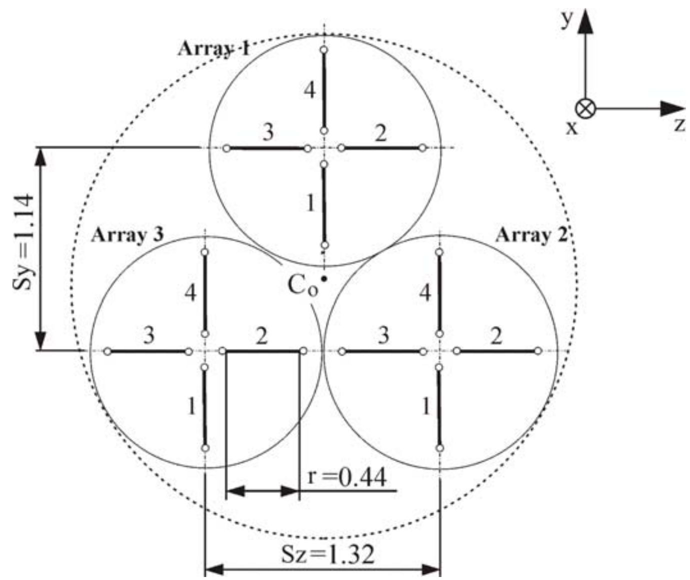

Dimensions in mm

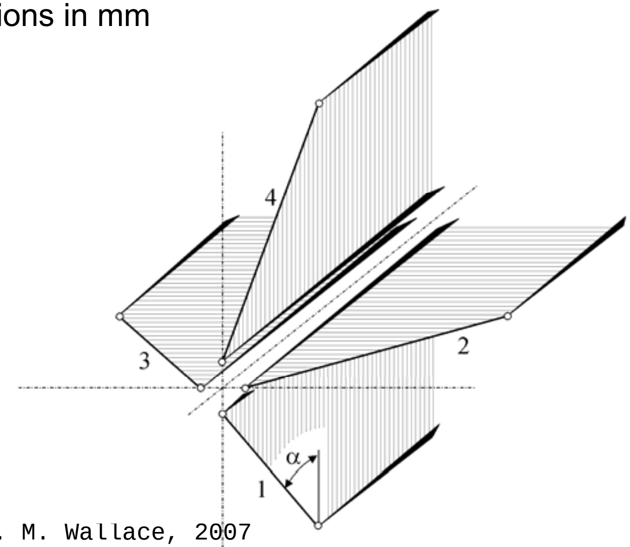

P.Vukoslavčević and J.M.Wallace (1996)

Meas. Sci. & Tech. 10

12-sensor Probe Data Processing

Taylor's series expansion of velocity components about probe cross-stream plane centroid to center of the jth sensor over the measured distances, C_j and D_j.

$$U_{1_j} = U_{1_o} + C_j \frac{\partial U_1}{\partial y} + D_j \frac{\partial U_1}{\partial z}$$

$$U_{2_j} = U_{2_o} + C_j \frac{\partial U_2}{\partial y} + D_j \frac{\partial U_2}{\partial z}$$

$$U_{3_j} = U_{3_o} + C_j \frac{\partial U_3}{\partial y} + D_j \frac{\partial U_3}{\partial z}$$

12 Cooling equations for each of the j sensors in terms of the three velocity components at the probe centroid and the six velocity gradients in the cross-stream plane.

$$P_j = A_{1_j} + A_{2_j} E_j + A_{3_j} E_j^2 + A_{4_j} E_j^3 + A_{5_j} E_j^4$$

is a polynomial of the measured voltages, Ej.

120 calibration coefficients, A_{ij} and k_{ij} to be determined .

$$\begin{aligned} f_j \equiv &- P_j + U_{1_o}^2 + 2C_j U_{1_o} \frac{\partial U_1}{\partial y} + 2D_j U_{1_o} \frac{\partial U_1}{\partial z} \\ &- k_{2j} \left[U_{2_o}^2 + 2C_j U_{2_o} \frac{\partial U_2}{\partial y} + 2D_j U_{2_o} \frac{\partial U_2}{\partial z} \right] \\ &- k_{3j} \left[U_{3_o}^2 + 2C_j U_{3_o} \frac{\partial U_3}{\partial y} + 2D_j U_{3_o} \frac{\partial U_3}{\partial z} \right] \\ &- k_{4j} \left[U_{1_o} U_{2_o} + C_j \left(U_{1_o} \frac{\partial U_2}{\partial y} + U_{2_o} \frac{\partial U_1}{\partial y} \right) + D_j \left(U_{1_o} \frac{\partial U_2}{\partial z} + U_{2_o} \frac{\partial U_1}{\partial z} \right) \right] \\ &- k_{5j} \left[U_{1_o} U_{3_o} + C_j \left(U_{1_o} \frac{\partial U_3}{\partial y} + U_{3_o} \frac{\partial U_1}{\partial y} \right) + D_j \left(U_{1_o} \frac{\partial U_3}{\partial z} + U_{3_o} \frac{\partial U_1}{\partial z} \right) \right] \\ &- k_{6j} \left[U_{2_o} U_{3_o} + C_j \left(U_{2_o} \frac{\partial U_3}{\partial y} + U_{3_o} \frac{\partial U_2}{\partial y} \right) + D_j \left(U_{2_o} \frac{\partial U_3}{\partial z} + U_{3_o} \frac{\partial U_2}{\partial z} \right) \right] = 0 \end{aligned}$$

System of equations solved by minimizing the error function $\sum f_j = 0$ iteratively at each time step.

Dissipation Rate in Near-Surface of Atmospheric Boundary Layer

Dugway site southwest of Salt Lake City

$R_\theta \approx 10^6$

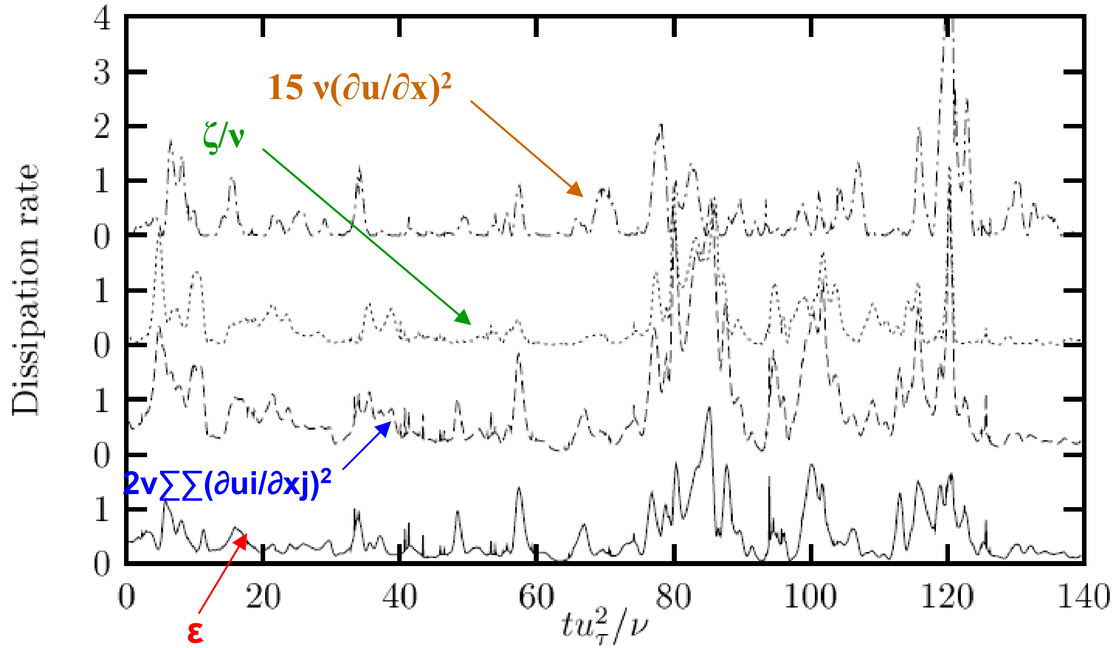

Folz (1997) Ph.D. Diss., Univ. of Maryland

An experimental study of the near-surface turbulence in the atmospheric boundary layer.

Dual Plane PIV Measurements of Dissipation Rate in a Turbulent Jet

J.A. Mullin & W.J.A. Dahm (2006)
Phys. Fluids 18

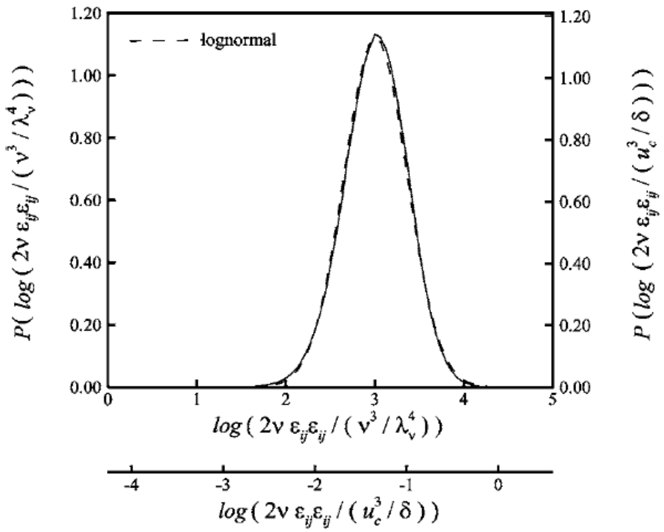

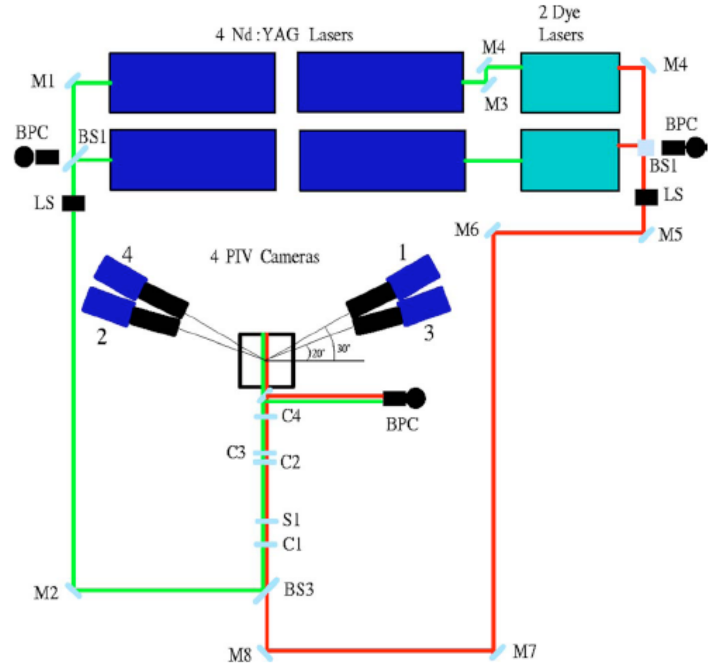

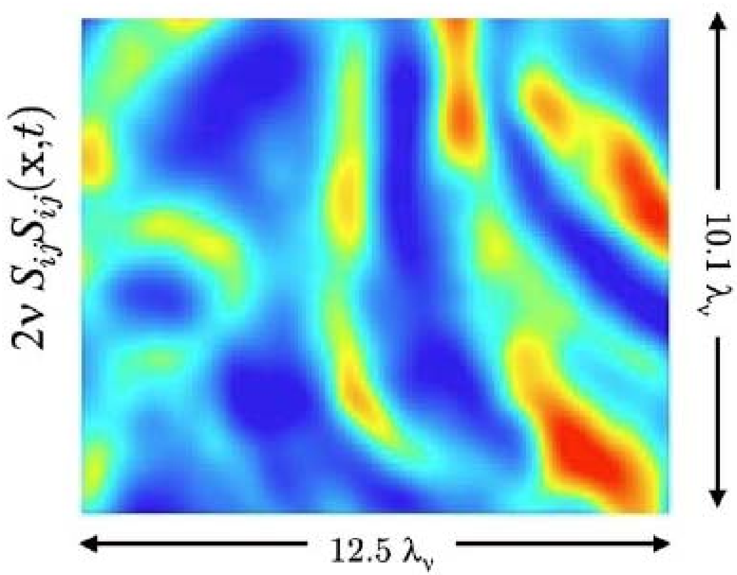

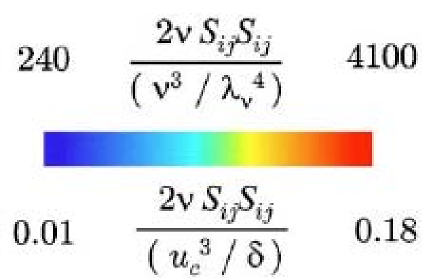

Visualization of Enstrophy and Dissipation Rate in a Channel Flow DNS

Iso-surfaces of enstrophy

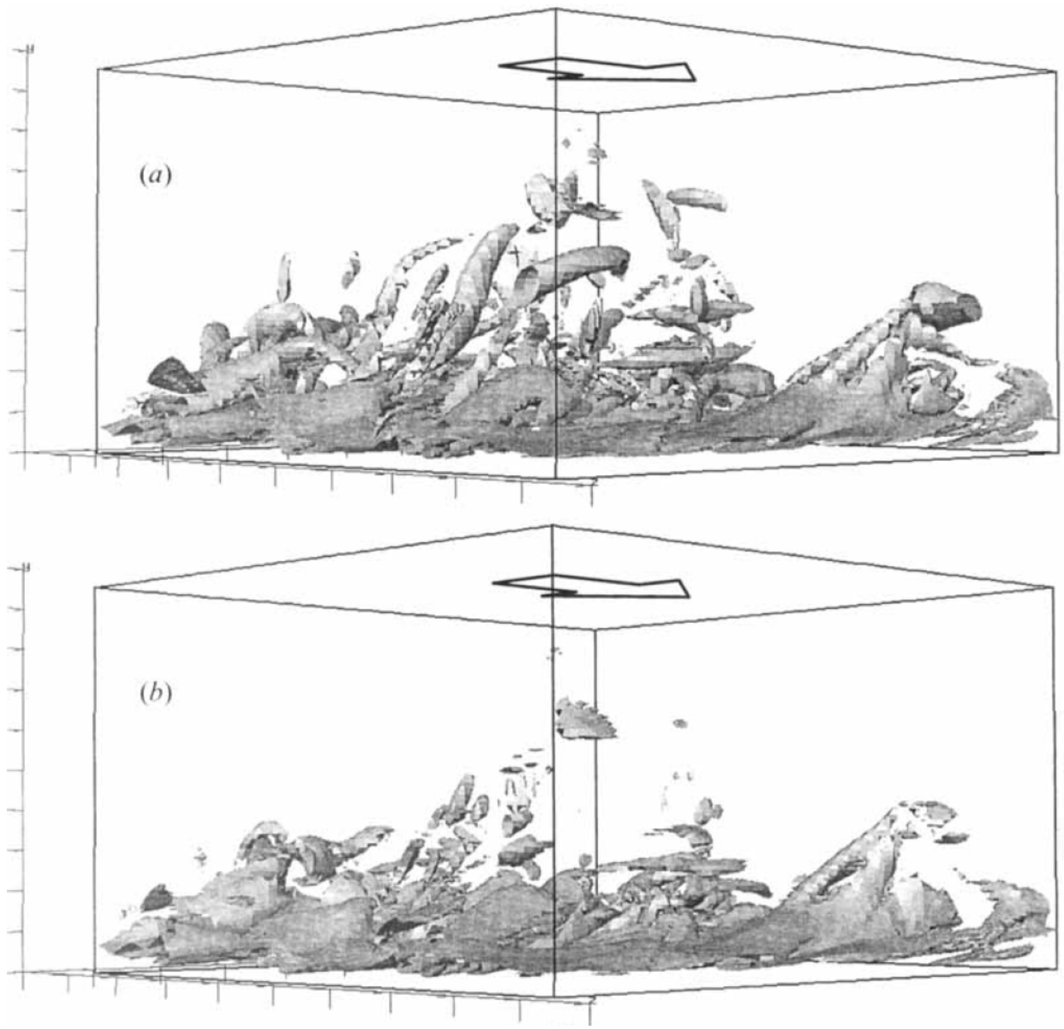

Iso-surfaces of dissipation rate

$\varepsilon = \nu\xi$ for homogeneous turbulence

Blackburn, N.N. Mansour & B.J. Cantwell (1996) JFM 310

Box of size $\Delta x^+ = 670$, $\Delta y^+ = 375$, $\Delta z^+ = 640$

Local Isotropy of the Vorticity Field in a High Reynolds Number Turbulent Boundary Layer

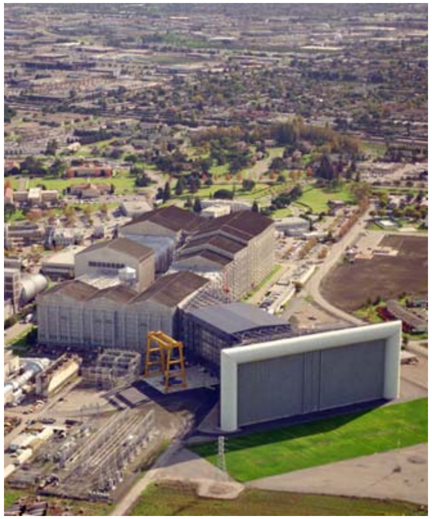

NASA Ames 80´ x 120´ Wind Tunnel

probe location

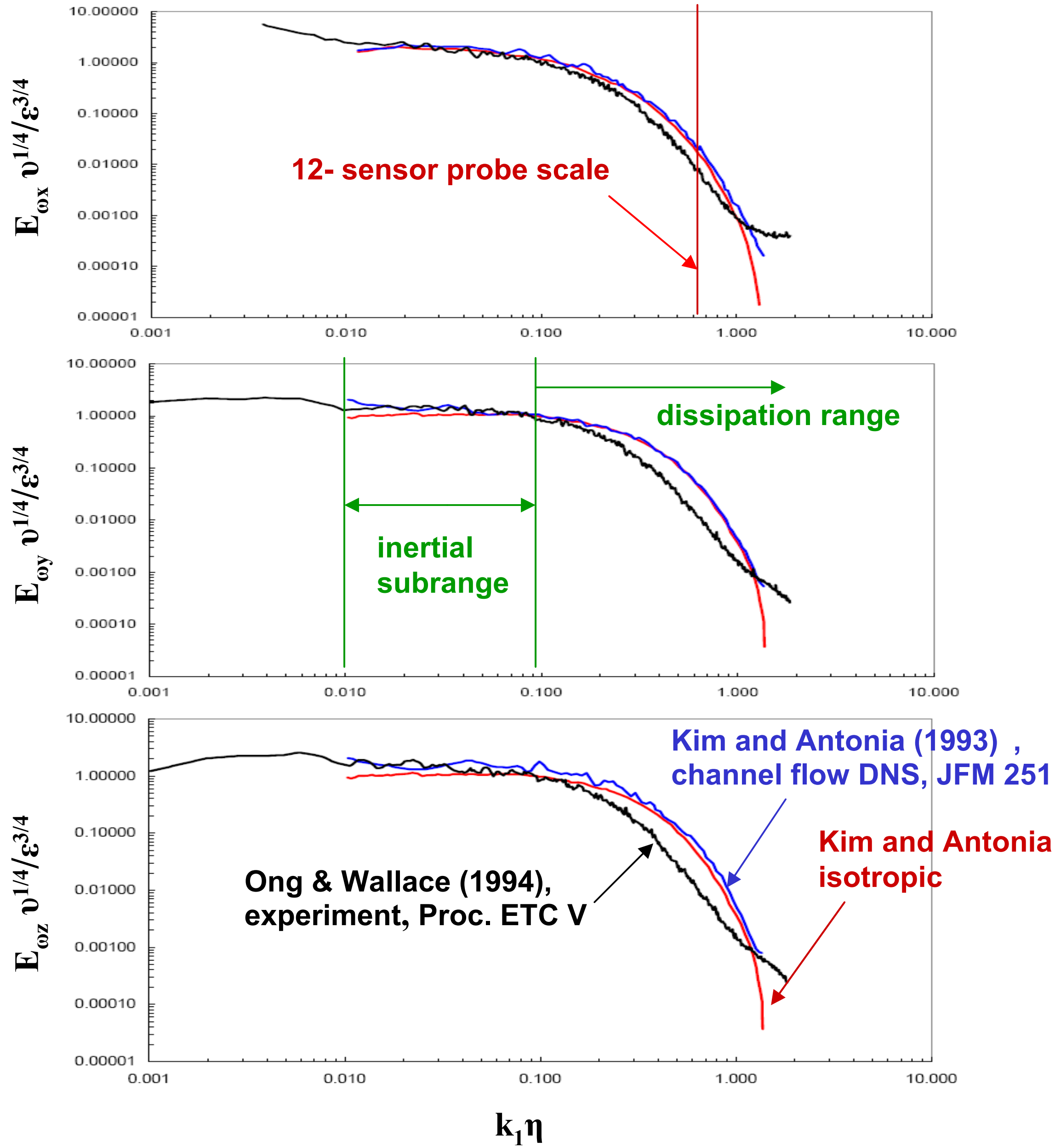

Orientation of the Vorticity Vector in Homogeneous Turbulent Shear Flow

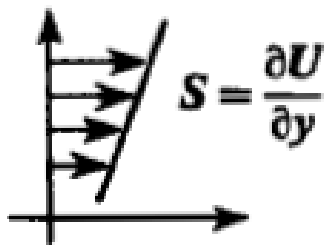

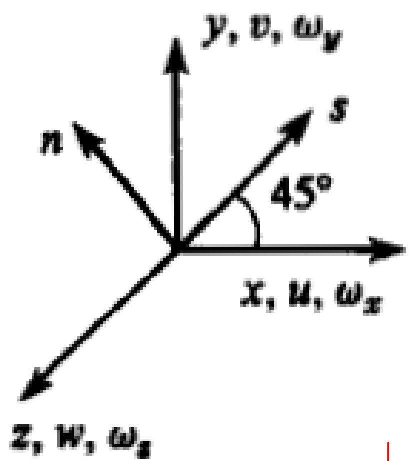

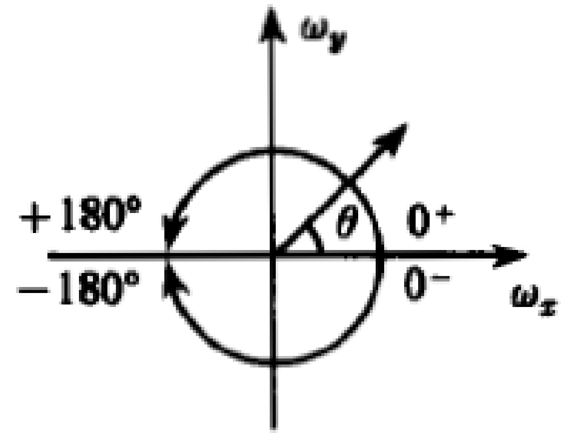

The distribution of the inclination angle of the projection of the vorticity vectors in the x-y streamwise plane. Data weighted with the magnitude of the projected vorticity $(\Omega_x^2 + \Omega_y^2)^{½}$.

Distribution attains rather sharp maxima at 45° and - 135° (the direction of principal elongation by the mean strain). R_λ = 14.2

M. M. Rogers & P. Moin (1987), JFM 176

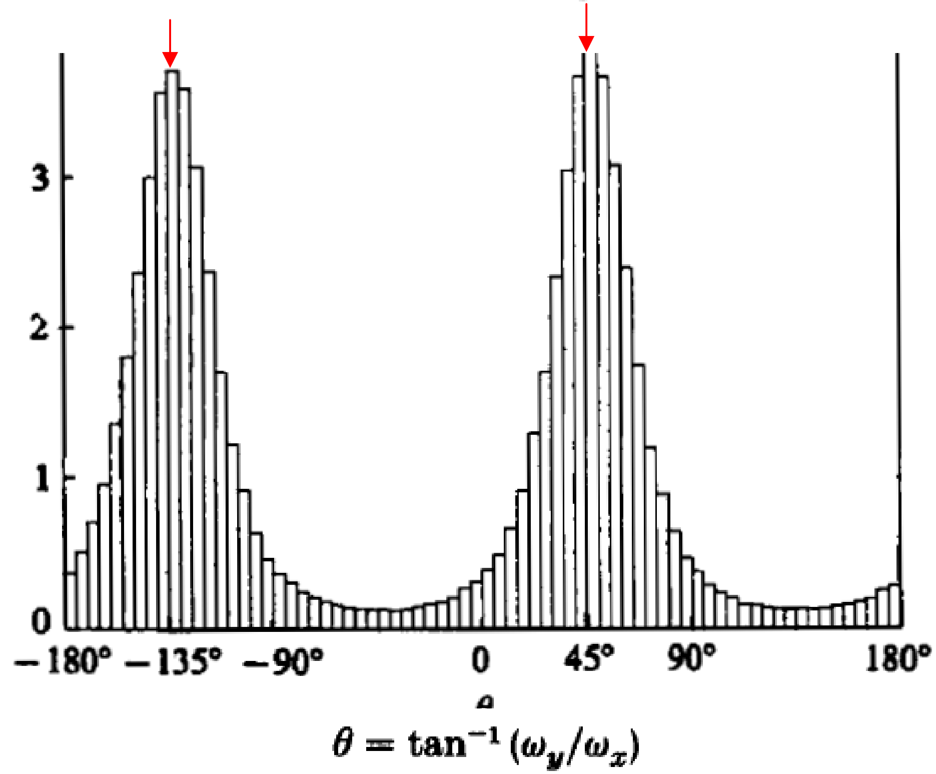

Vortex Lines and Vorticity Component Correlation

Two-point correlation of ω_s vorticity component with spanwise separation

$R_{\omega s \omega s}$

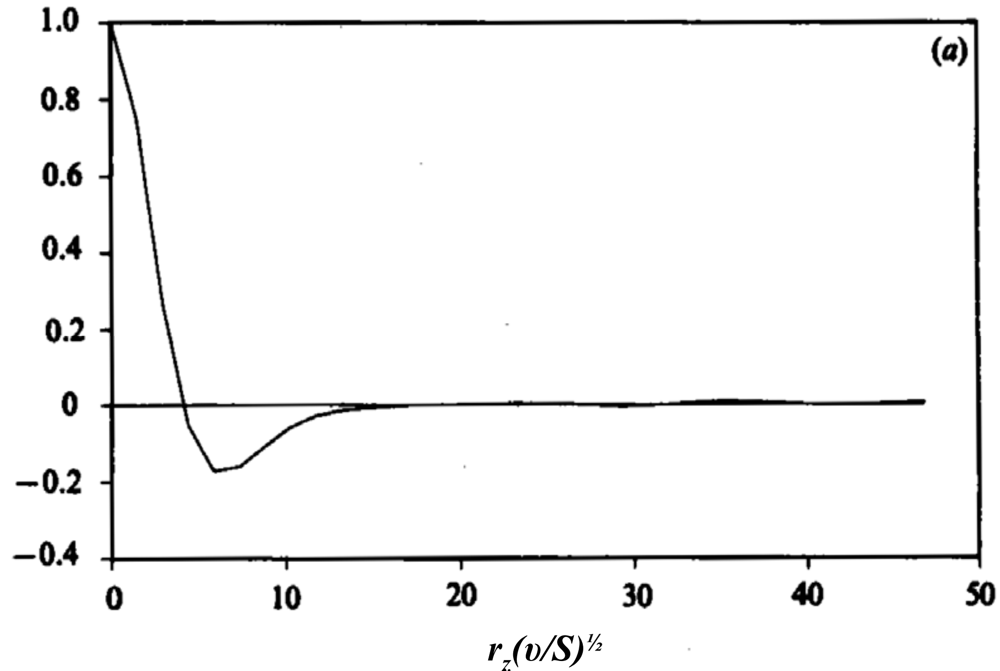

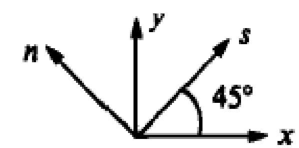

Hairpin Shaped vortex Lines

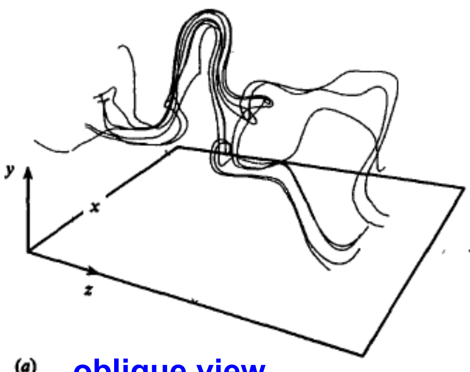

oblique view

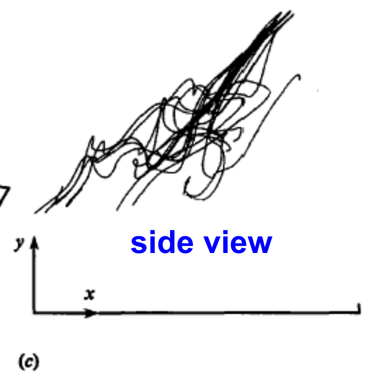

side view

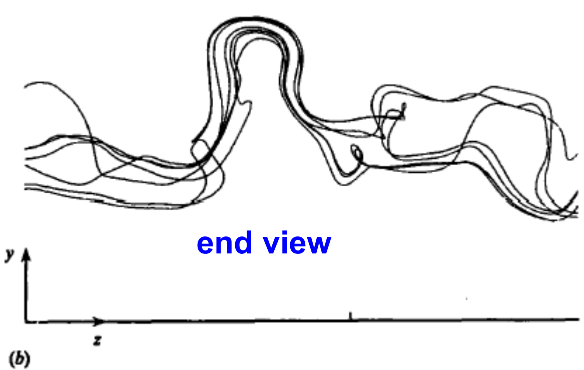

end view

M. M. Rogers & P. Moin
(1987)
JFM 176

Orientation of the Vorticity Vector in a Turbulent Boundary Layer

JPDFs

$P(\Omega_x, \Omega_y)$

Streamwise x-y Plane

Covariance Integrands
$\Omega_x \Omega_y P(\Omega_x, \Omega_y)$

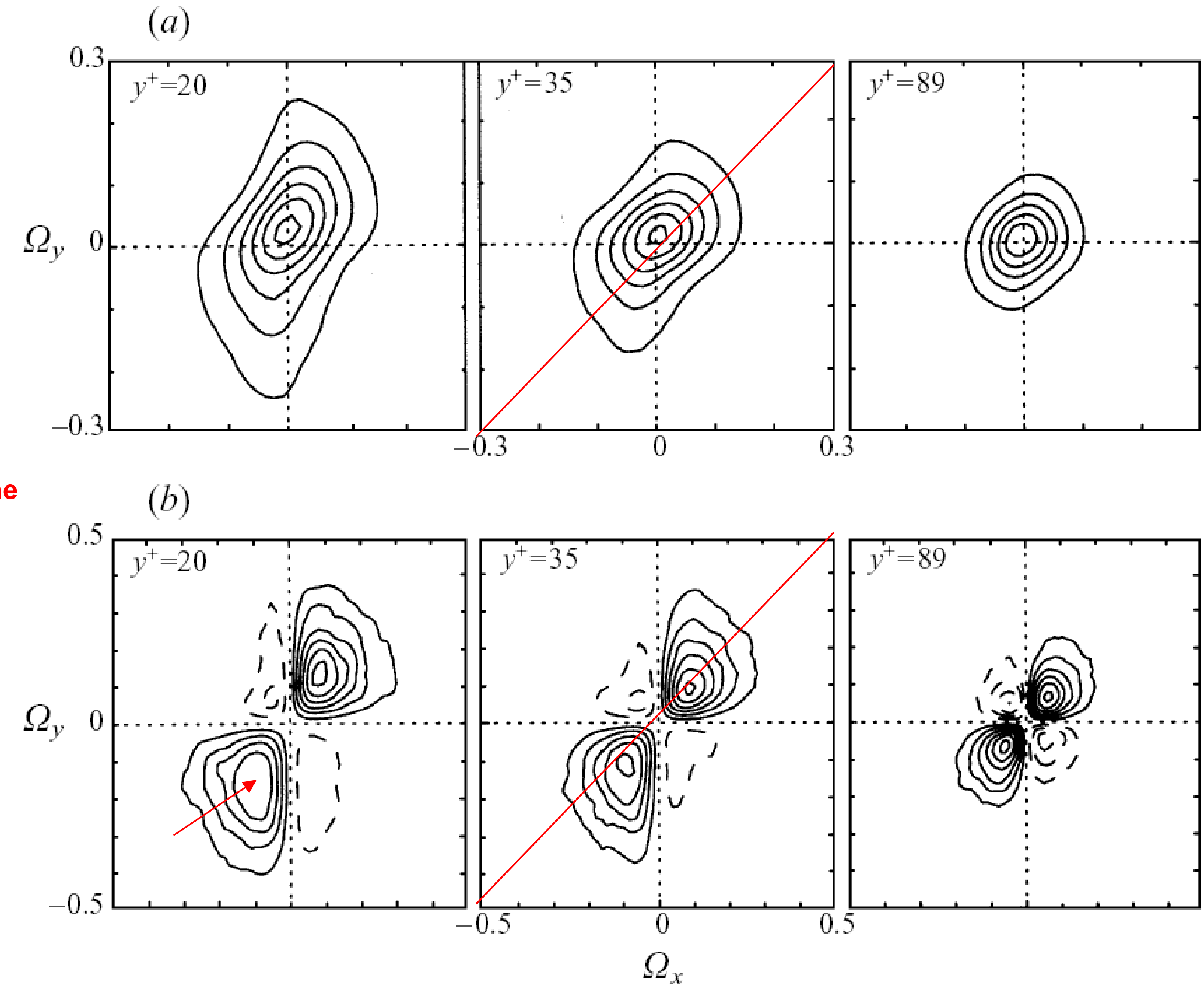

L. Ong & J.M. Wallace (1998) JFM 367

Vorticity Filaments and Vorticity Covariances

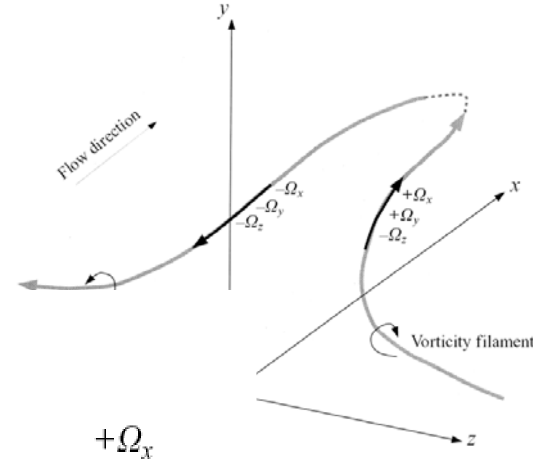

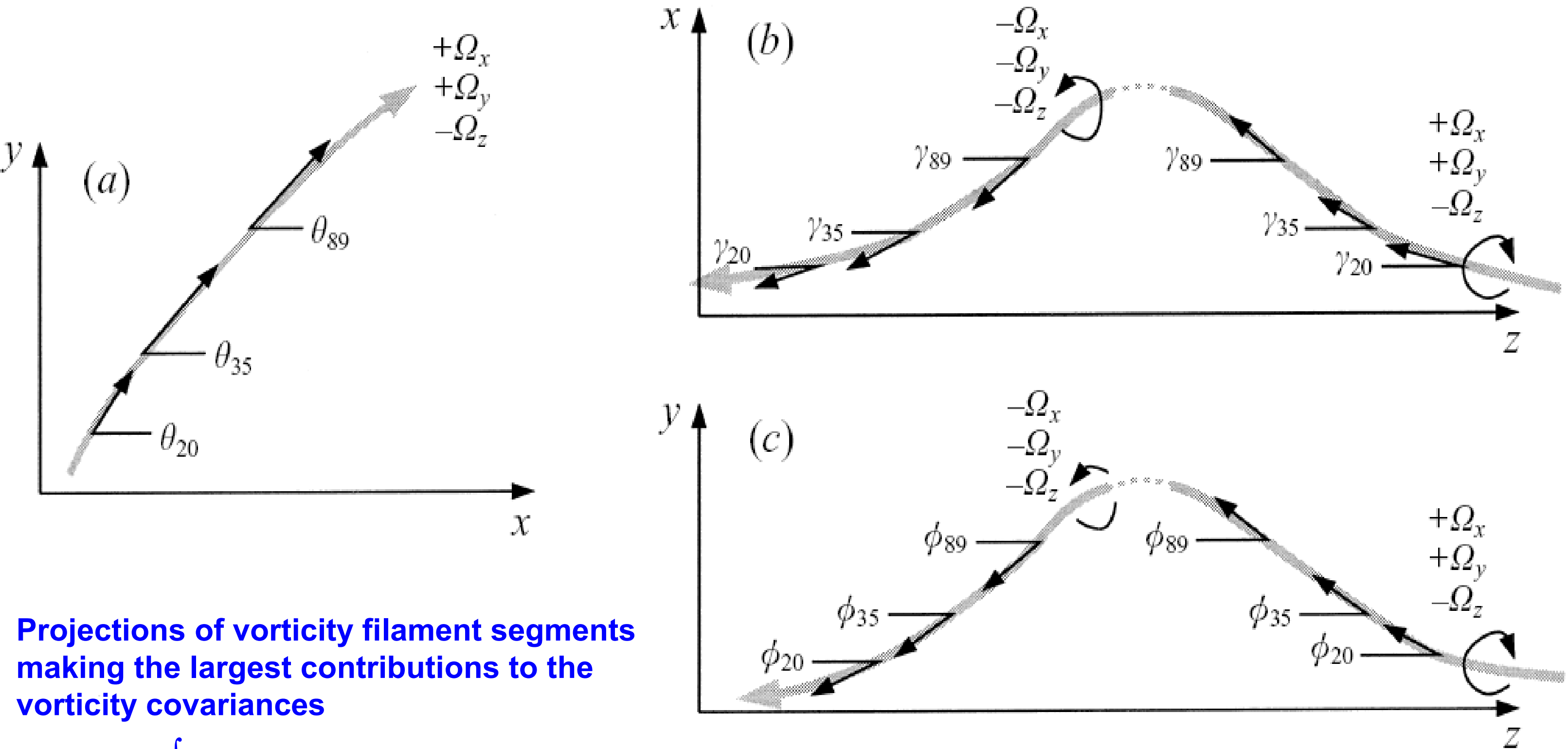

Projections of vorticity filament segments making the largest contributions to the vorticity covariances

$$\langle \Omega_x \Omega_y \rangle = \int \Omega_x \Omega_y P(\Omega_x, \Omega_y)\, d\Omega_x\, d\Omega_y$$

L. Ong & J.M. Wallace (1998) JFM 367

PIV Study of Vortices in a Turbulent Boundary Layer

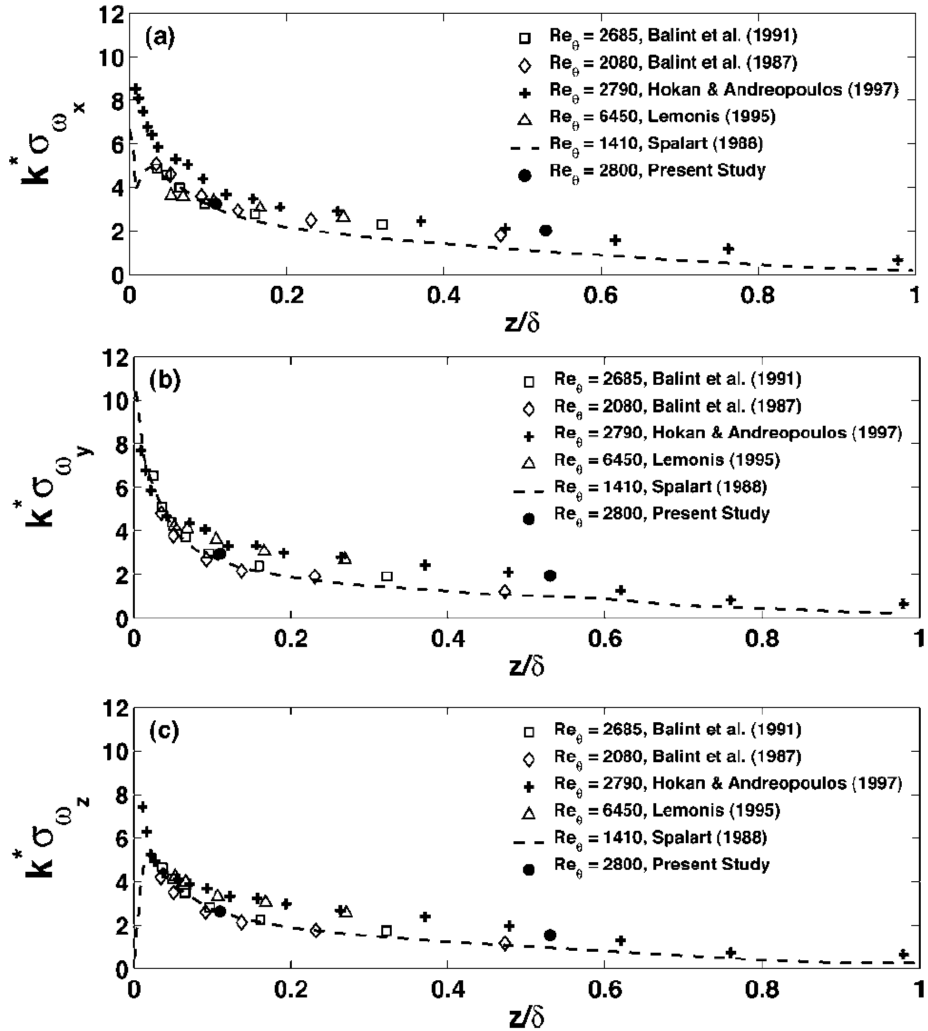

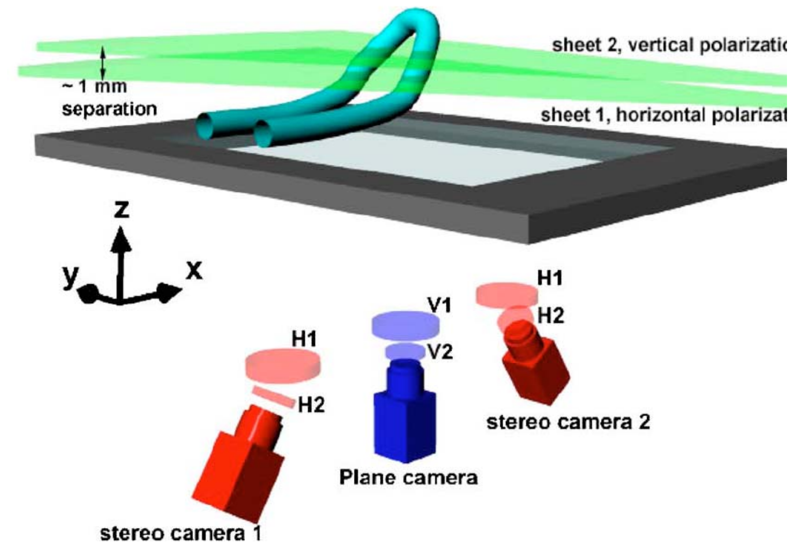

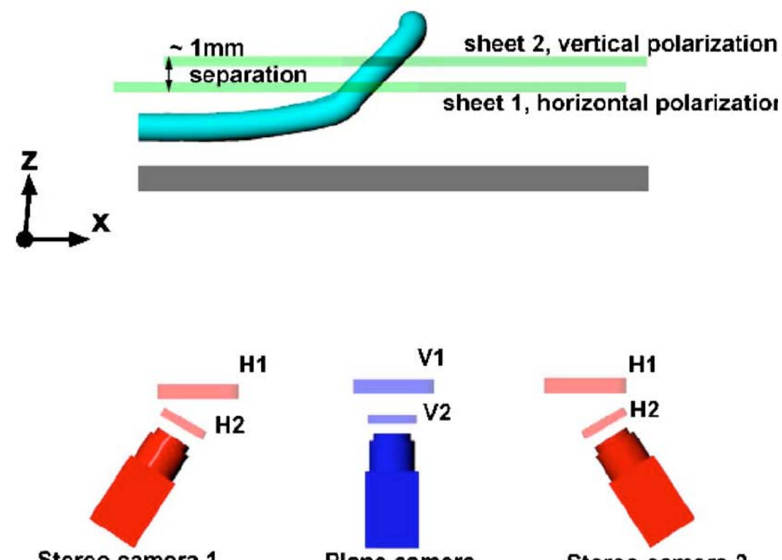

B. Ganapathisubramani, E. Longmire & I. Marusic

Phys. Fluids 18 (2006)

PIV Study of Vortices in a Turbulent Boundary Layer

B. Ganapathisubramani, E. Longmire & I. Marusic
Phys. Fluids 18 (2006)

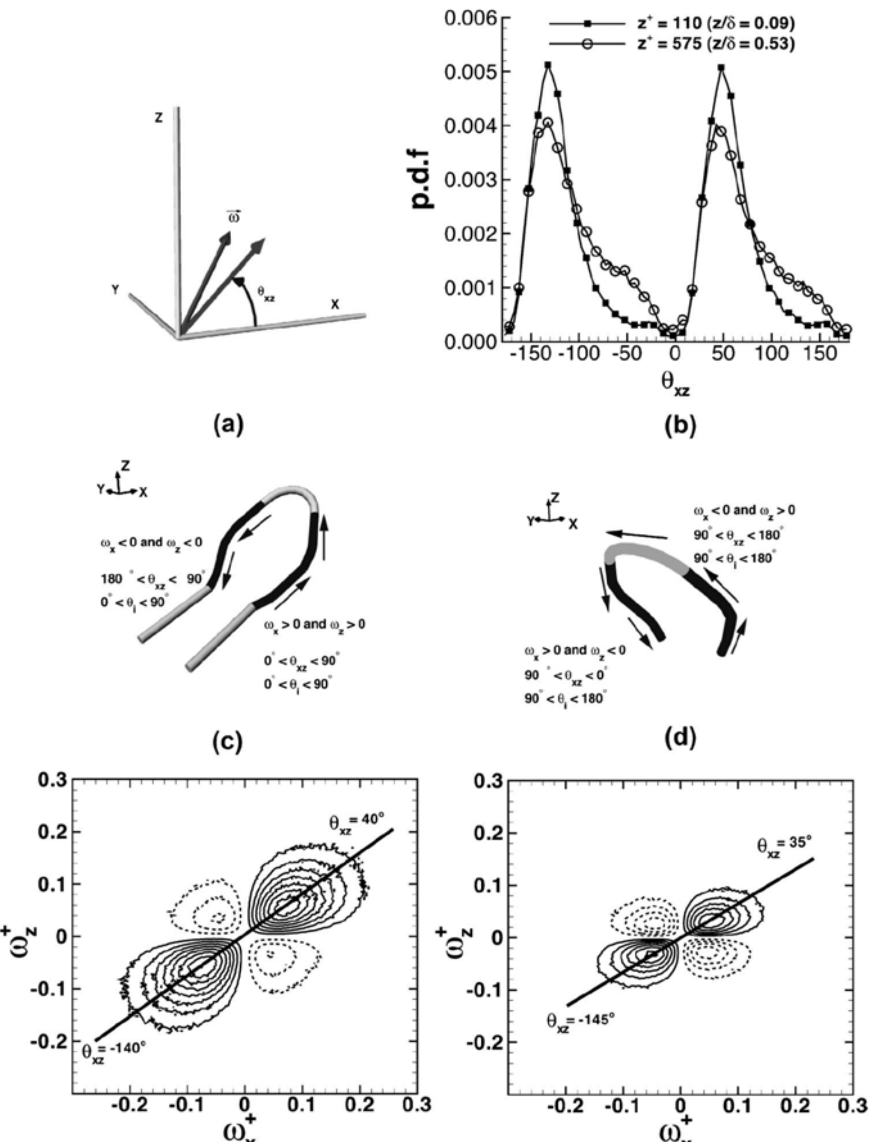

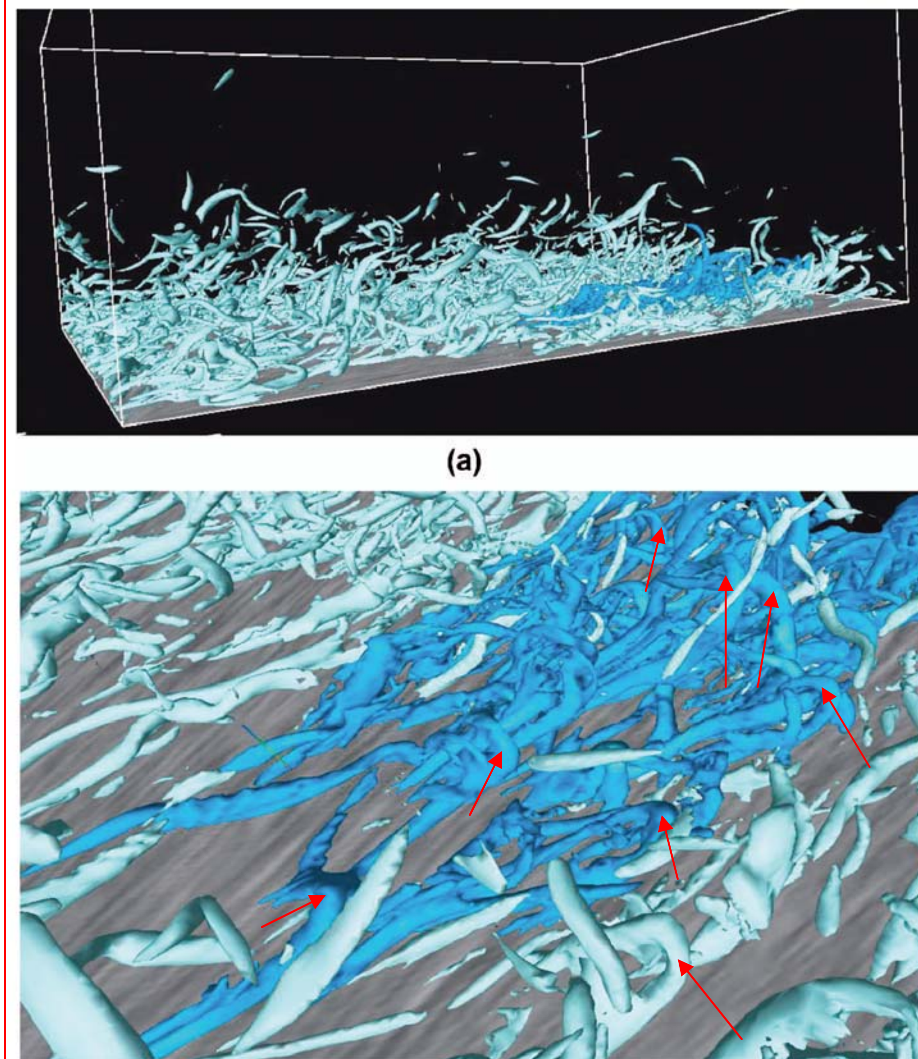

Δ vortex identifier applied to channel flow DNS of
J. Del Alamo, J. Jimenez, P. Zandonade & R. Moser
J. Fluid Mech. 500 (2004)

Alignment of Vorticity Vector with Eigenvectors of Rate-of-Strain Tensor

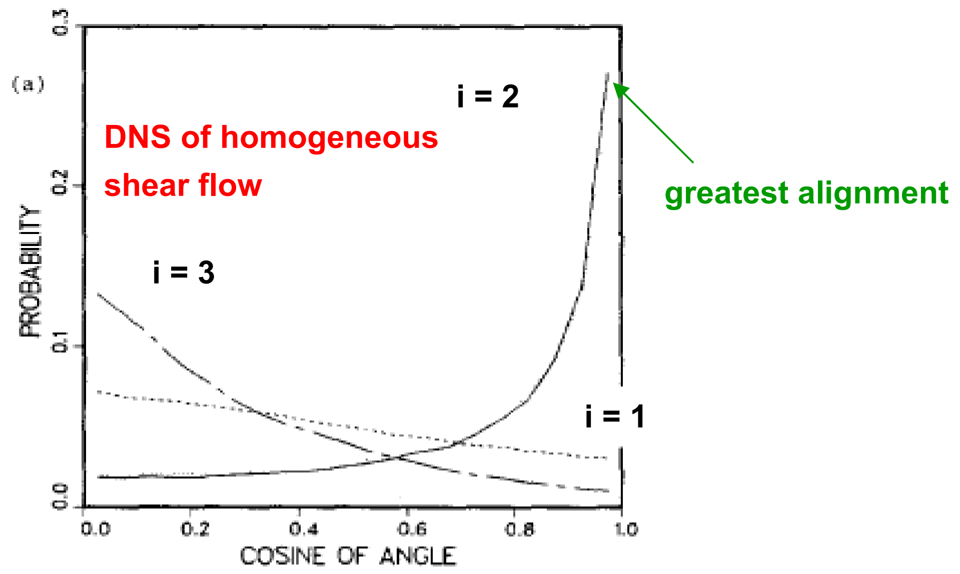

PDFs of cosine of angle between vorticity vector and eigenvectors of the rate-of-strain tensor, α_i

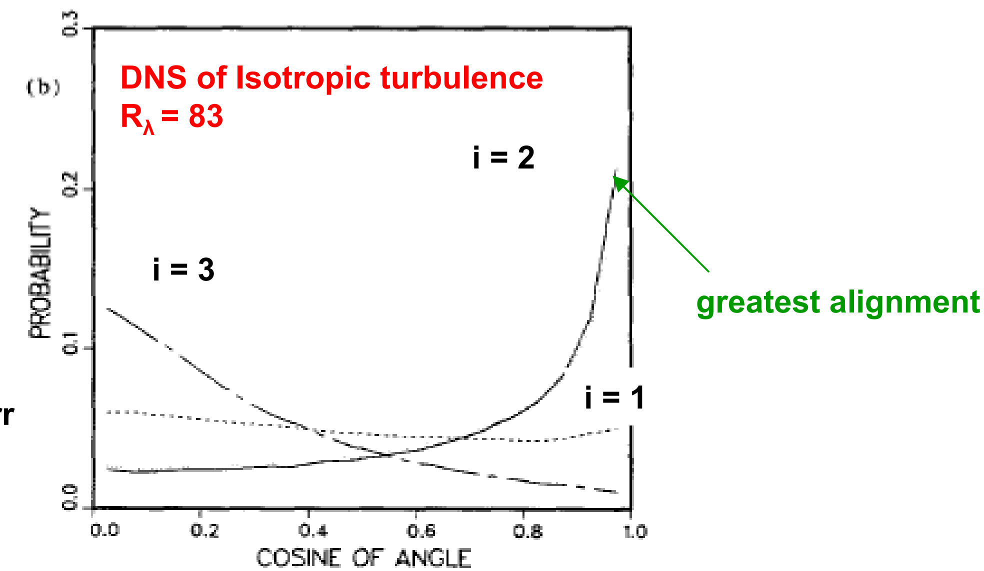

Wm. T. Ashurt, A. R. Kerstein, R. M. Kerr and C. H. Gibson (1987) Phys. Fluids 30

12-Sensor Hot-Wire Probe

(a)

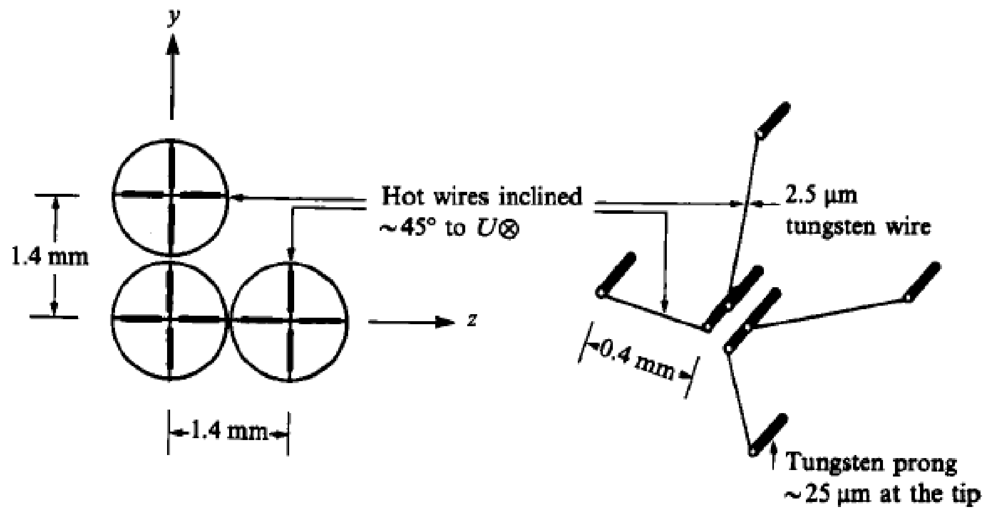

(b)

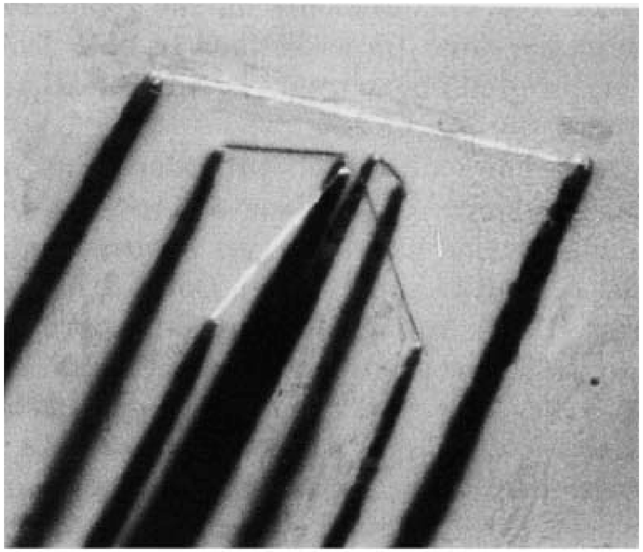

Tsinober, E. Kit & T. Dracos (1992)
JFM 242

Alignment of Vorticity Vector with Eigenvectors of Rate-of-Strain Tensor

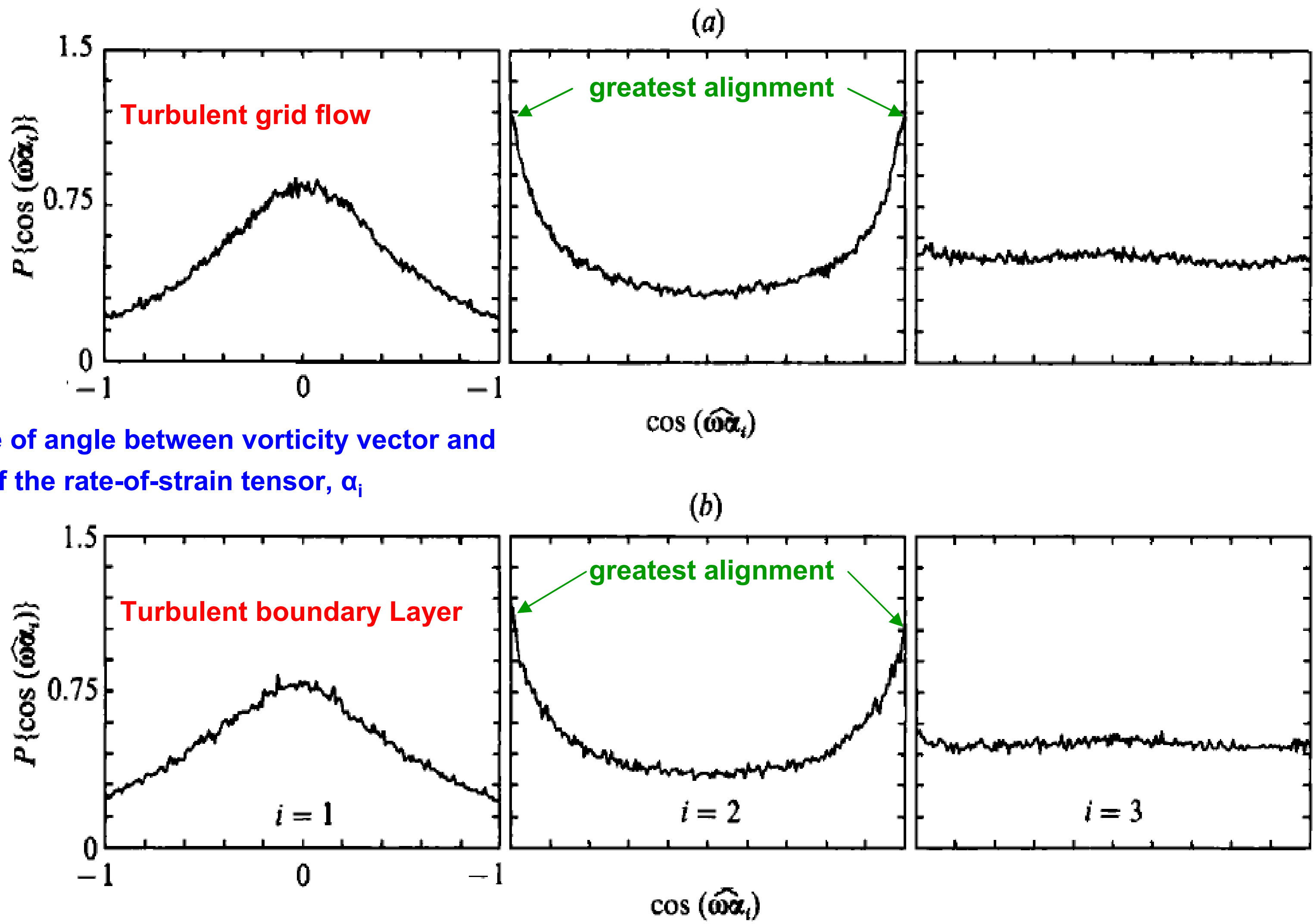

PDFs of cosine of angle between vorticity vector and eigenvectors of the rate-of-strain tensor, α_i

Tsinober, E. Kit & T. Dracos (1992) JFM 222

Alignment of Vorticity Vector with Eigenvectors of Rate-of-Strain Tensor

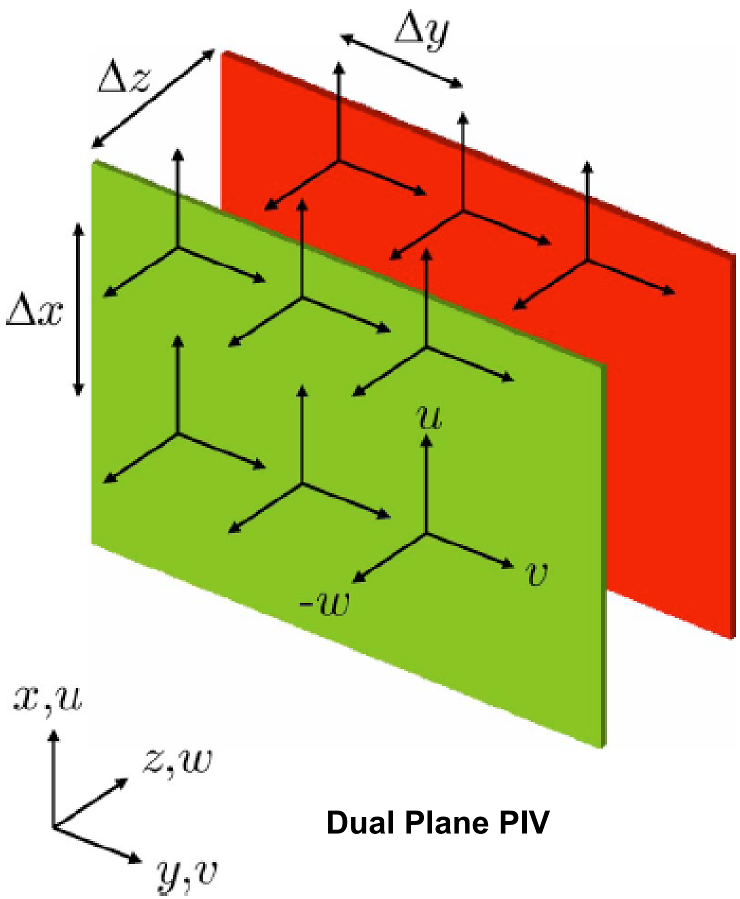

Dual Plane PIV

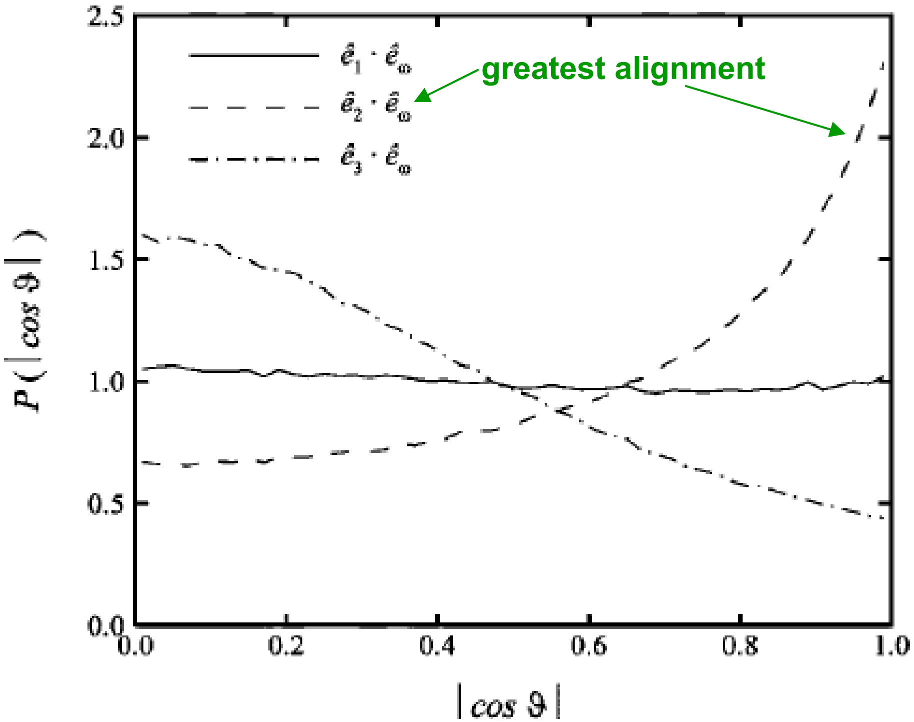

J.A. Mullin & W.J.A. Dahm (2006)

Phys. Fluids 18

JPDF of the Q and R invariants of the Velocity Gradient Tensor A_{ij}

$A_{ij} = \partial U_i/\partial x_j = S_{ij} + R_{ij}$ (velocity gradient tensor)

$S_{ij} = \frac{1}{2}(\partial U_i/\partial x_j + \partial U_j/\partial x_i)$ (strain rate)

$R_{ij} = \frac{1}{2}(\partial U_i/\partial x_j - \partial U_j/\partial x_i)$ (rotation rate)

$\lambda^3 + P\lambda^2 + Q\lambda + R = 0$ (characteristic eqn of A_{ij})

$P = - S_{ii} = 0$ (for incompr. Flow)

$Q = \frac{1}{2}(- S_{ij}S_{ij} + R_{ij}R_{ij})$

$R = - \frac{1}{3}(S_{ij}S_{jk}S_{ki} + 3R_{ij}R_{jk}S_{ki})$

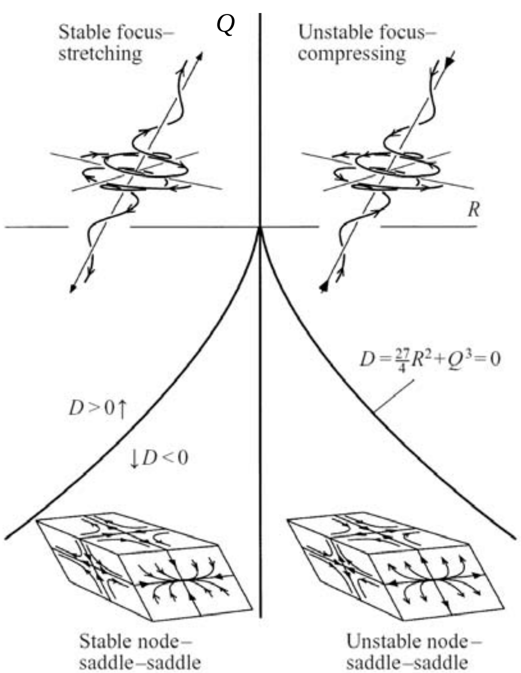

Data from throughout $R_\theta = 670$ boundary layer DNS of Spalart

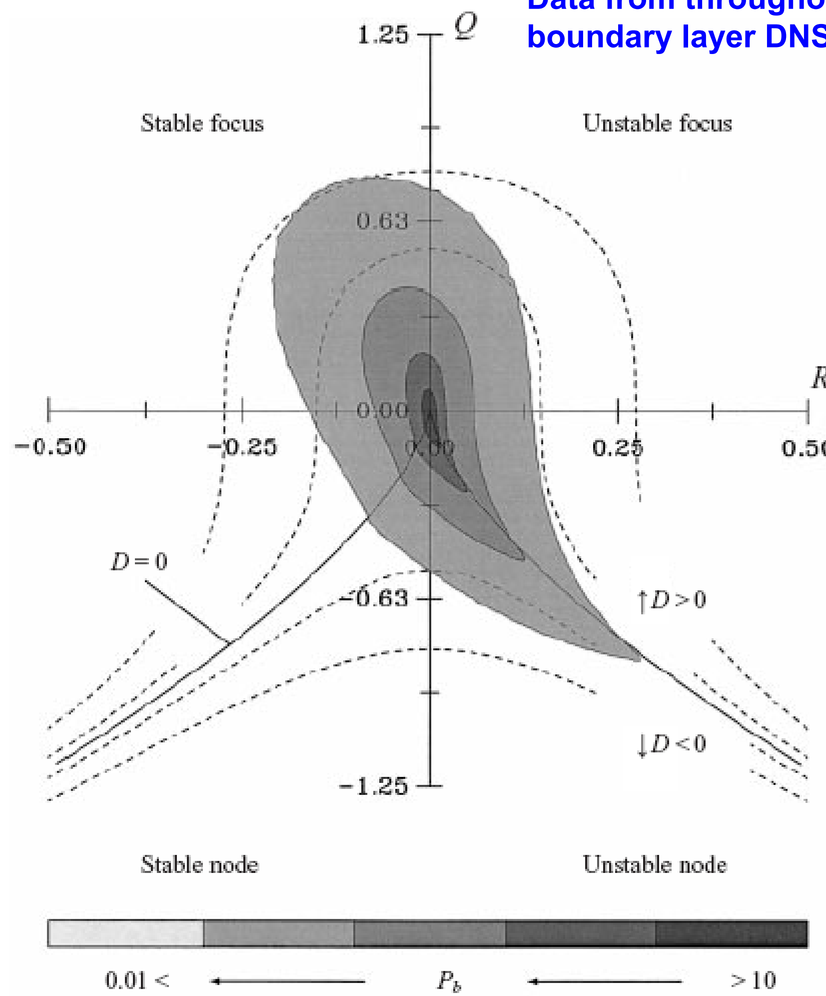

J.M. Chaćin & B. J. Cantwell (2000)
JFM 404

Reynolds Stress Associated with Incompressible Flow Patterns from the Q-R Invariants

Grey levels show Reynolds shear stress amplitudes associated with Q-R incompressible flow patterns

Data from throughout $R_\theta = 670$ boundary layer DNS of Spalart

J.M. Chaćin & B. J. Cantwell (2000)
JFM 404

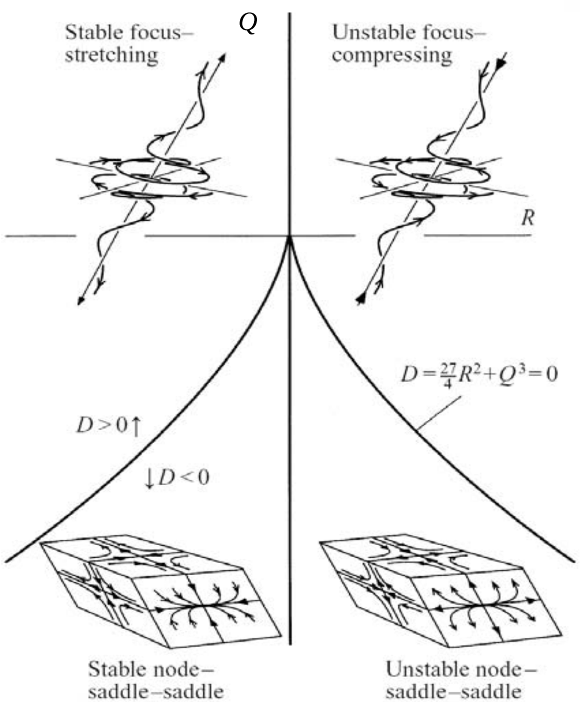

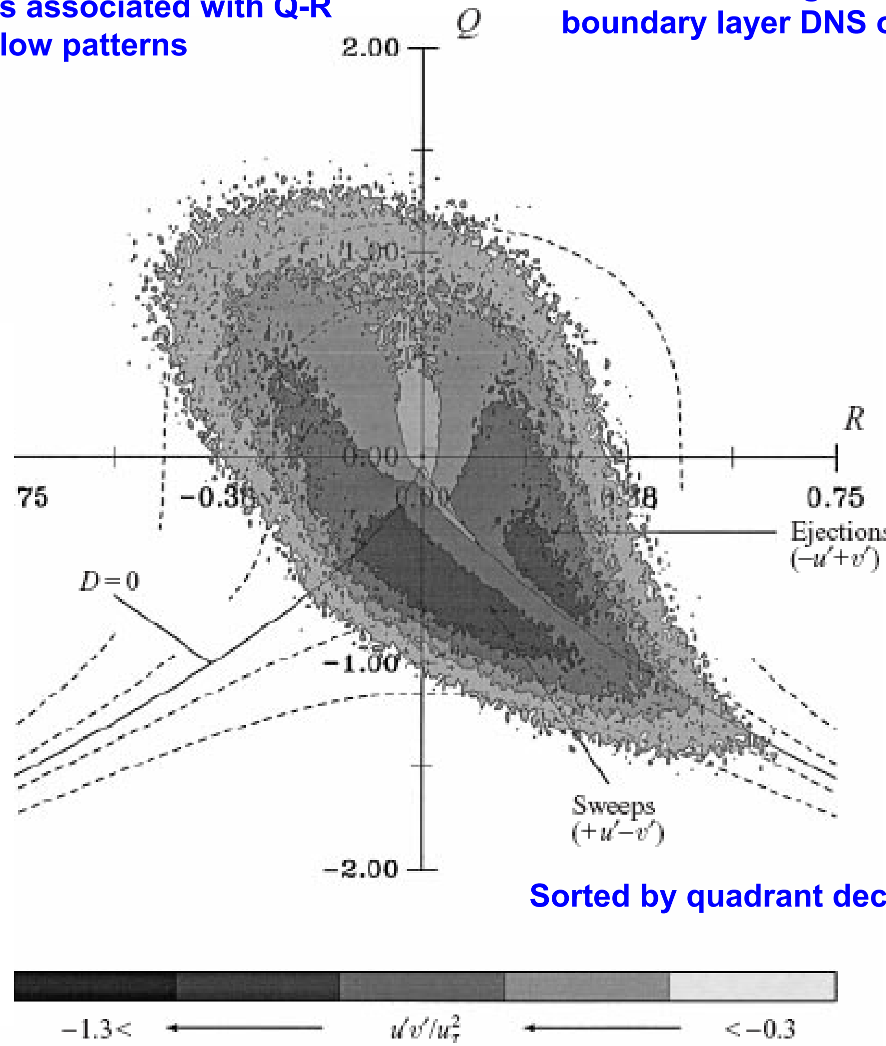

Sorted by quadrant decomposition

Nine-Sensor Hot-Wire Probe

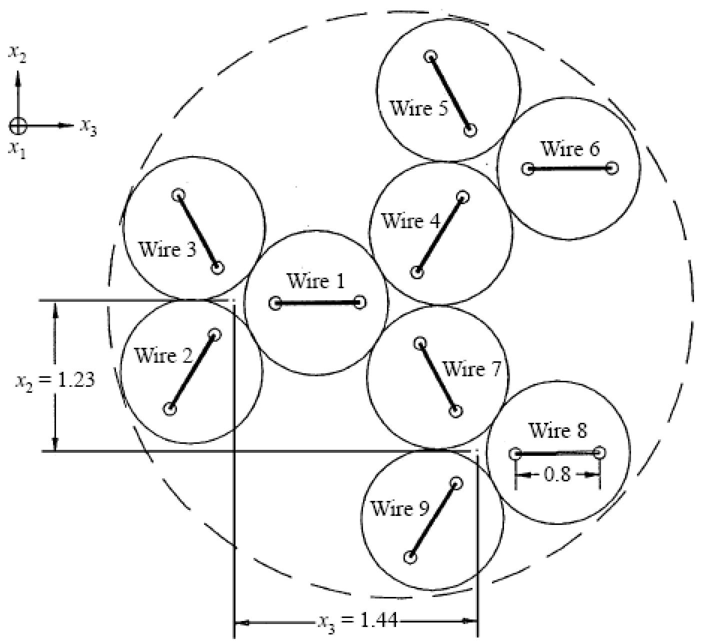

A. Honkan & Y. Andreopoulos (1997)
JFM 350

JPDF of the Q and R Invariants of the Velocity Gradient Tensor Aij

Y. Andreopoulos & A. Honkan (2001)
JFM 439

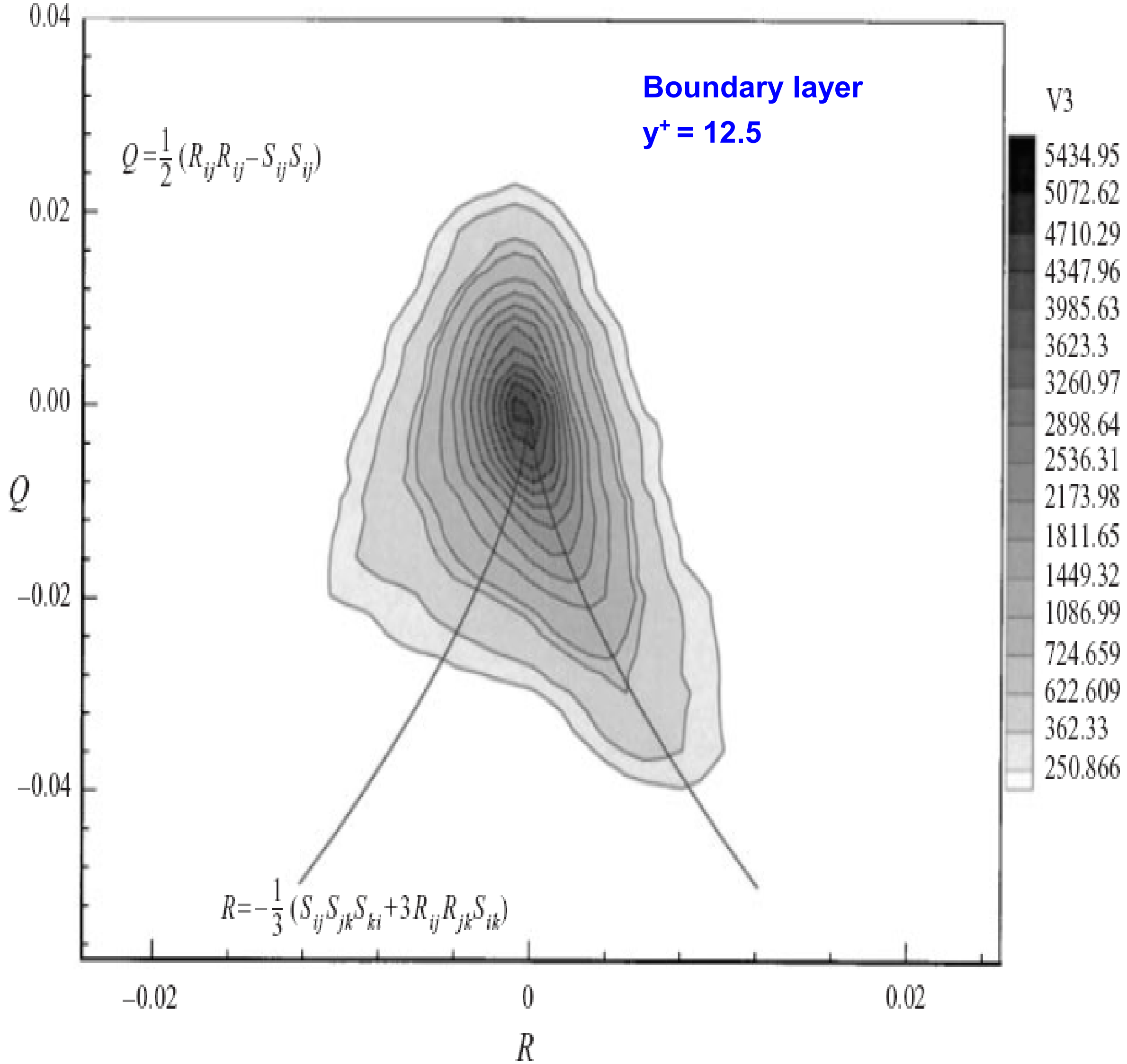

Vorticity Tubular "Worms" in Isotropic Turbulence

Vorticity field in DNS of isotropic turbulence at $R_\lambda = 150$. Vector length proportional to the vorticity magnitude at each grid point.

"Vorticity is organized in thin elongated tubes…Their thickness is of the order of a few dissipation scales…"

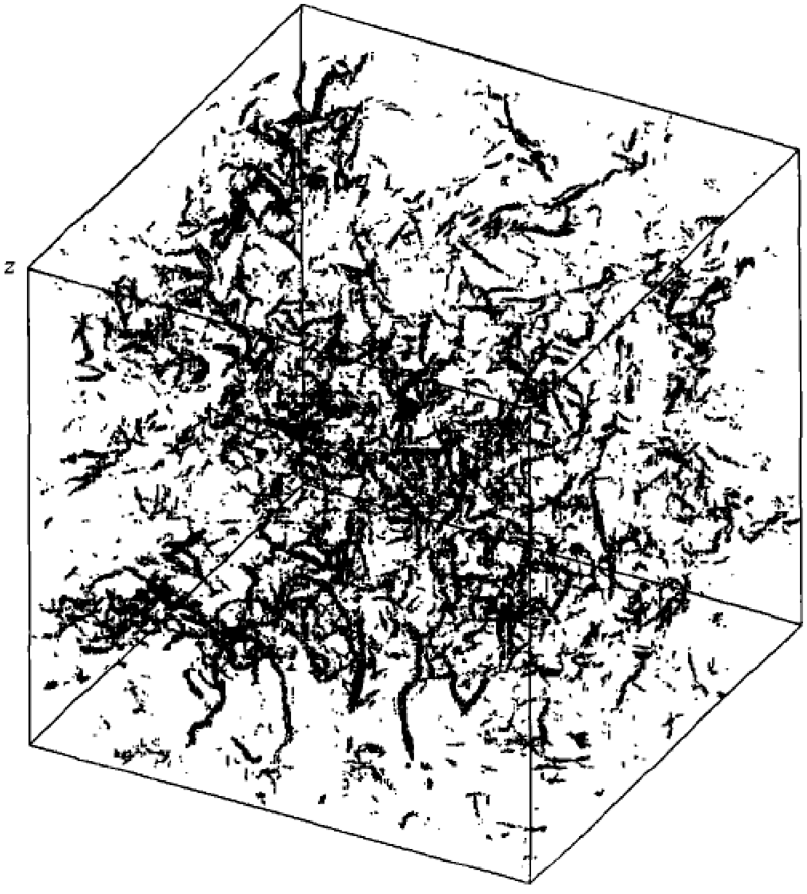

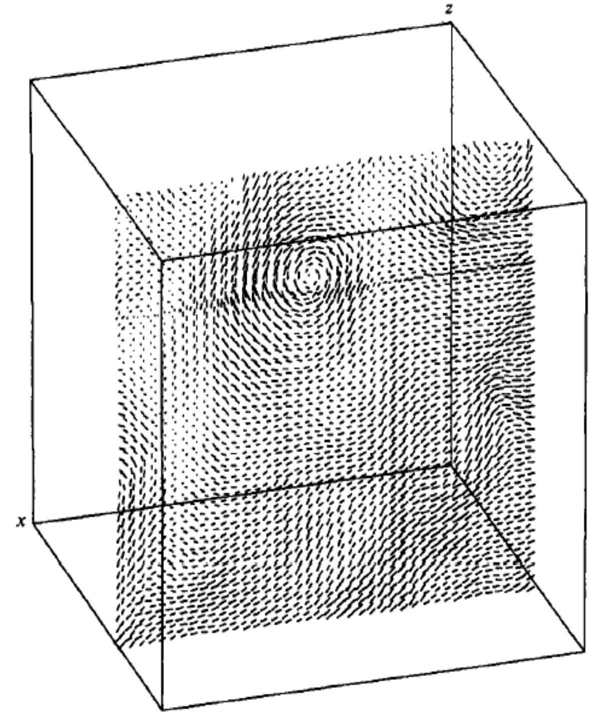

Projection of the velocity field perpendicular to a single vorticity tube

Vincent & M. Meneguzzi (1991)
JFM 225

Schemes for Vortex Identification based on Velocity Gradient Tensor

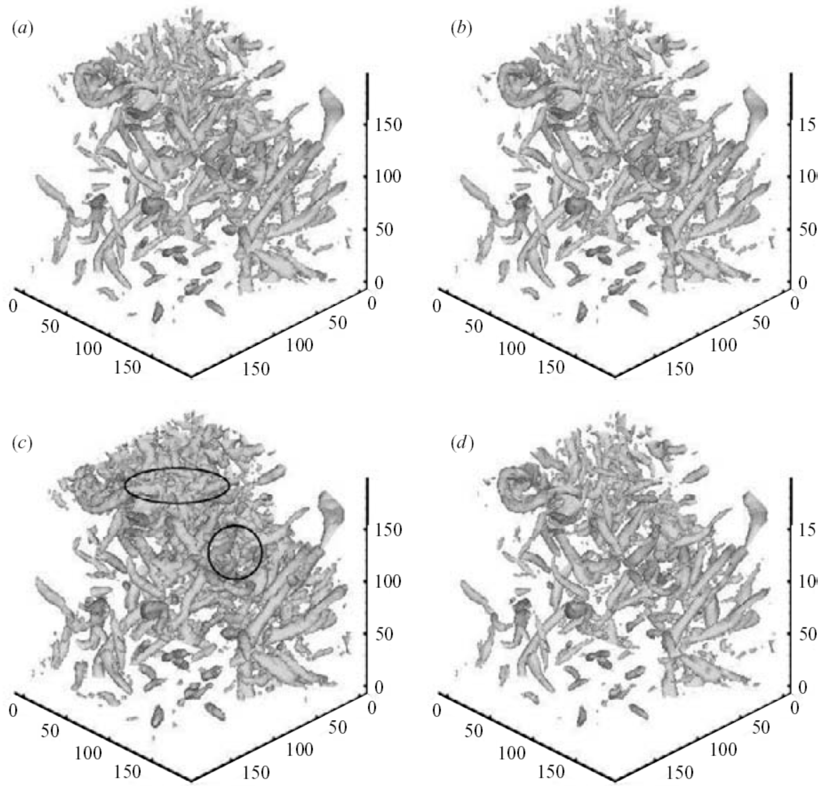

λ_{ci}, **Swirling strength,** Zhou et al. (1999) JFM 387

Q, Positive 2nd invariant, Hunt et al. (1988), CTR –S88

Δ, complex eigenvalues, Chong et al. (1990), Phys. Fluids A 2

λ_2, **local pressure minimum,** Jeong & Hussain (1985), JFM 285

Λ_2, **special case**

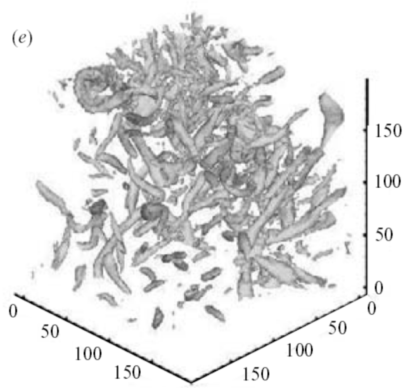

(f) R_λ = 150

Overlap volume	%
vol(λ_{ci}, Q)/vol(λ_{ci})	90.43
vol(λ_{ci}, Δ)/vol(Δ)	73.54
vol(λ_{ci}, λ_2)/vol(λ_{ci})	84.44
vol(λ_{ci}, λ_2)/vol(λ_2)	99.72
vol(Q, λ_2)/vol(λ_2)	98.65
vol(Q, λ_2)/vol(Q)	92.38
vol(λ_2, $\tilde{\lambda}_2$)/vol(λ_2)	99.58

P. Chakraborty, S. Balachandar & R. J. Adrian (2005), JFM 535

Animation of Vortex Structures in a Turbulent Boundary Layer

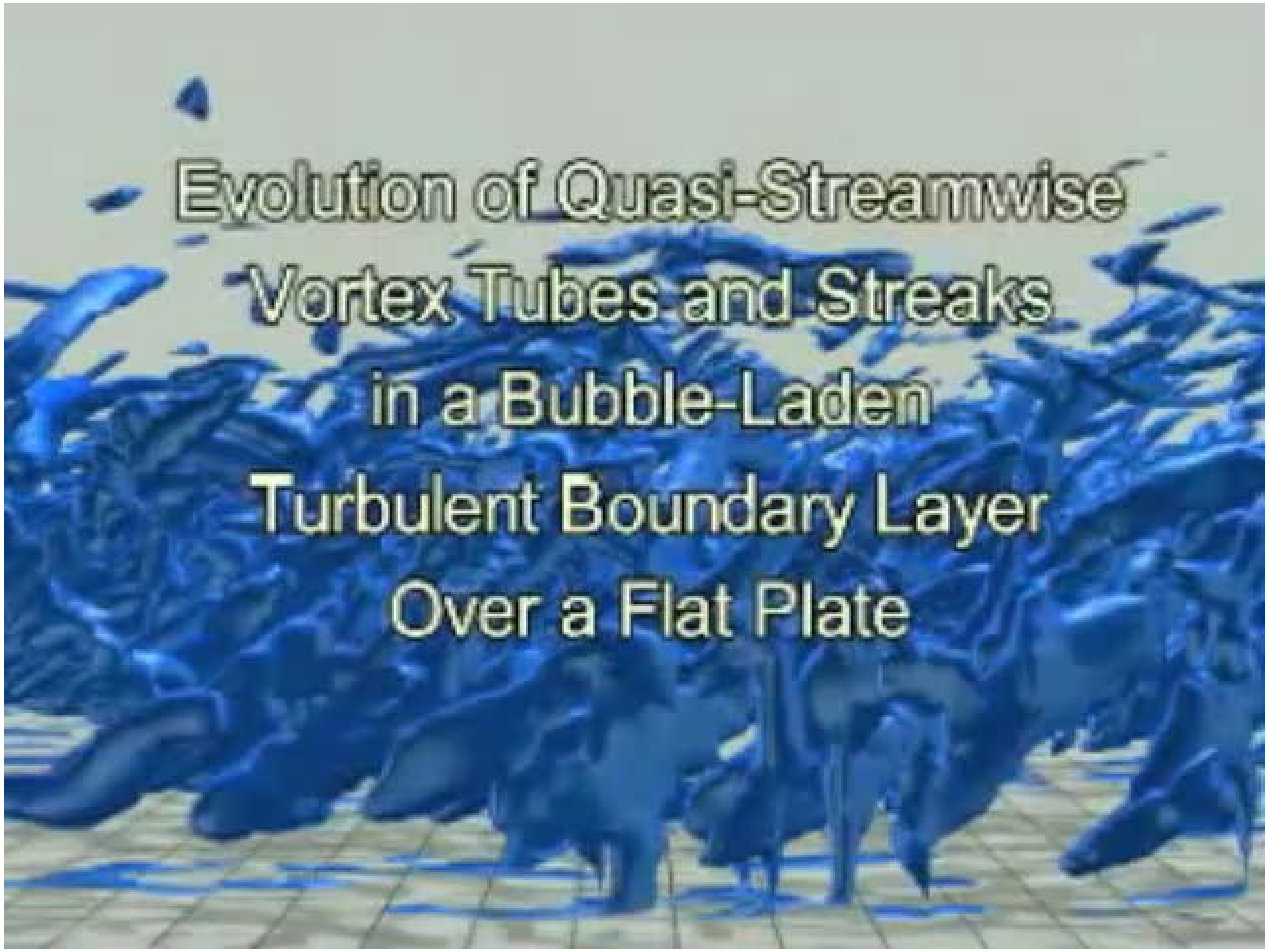

Vortex Identification with λ_2, local pressure minimum,
Jeong & Hussain (1985), JFM 285

Evolution of Quasistreamwise Vortex Tubes and Wall Streaks in a Bubble-laden Turbulent Boundary Layer over a Flat Plate
A. Ferrante, S. Elghobashi, P. Adams, M. Valenciano, and D. Longmire

Physics of Fluids

http://pof.aip.org/pof/gallery/video/2004/901406phf_15MB.mov

Generation and Evolution of a Hairpin Vortices in a DNS Channel Flow

Primary vortex extracted from the two-point spatial correlation of the velocity field by linear stochastic estimation given a second-quadrant ejection event vector

New vortices are generated upstream of the primary vortex

They also are generated downstream and to the side of the primary vortex

These clusters of vortices are known as packets

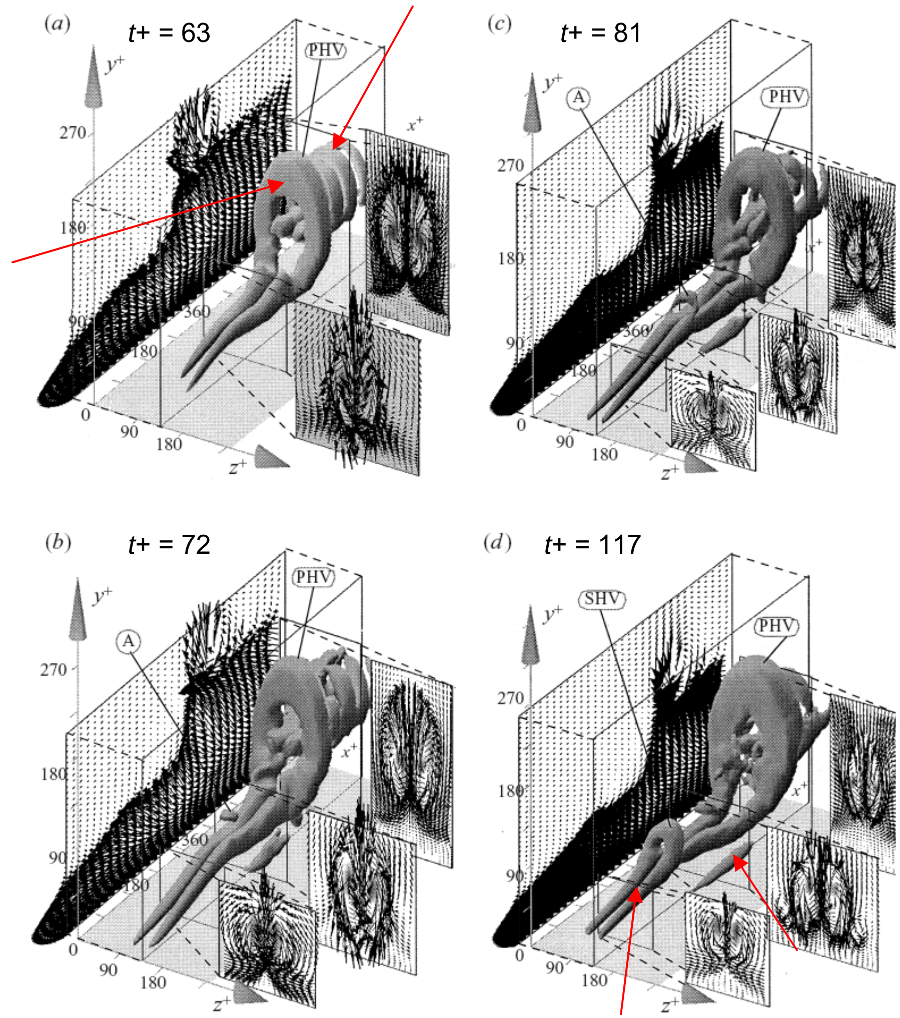

J. ZHOU, R. J. ADRIAN, S. BALACHANDAR &T. M. KENDALL (1999)
JFM 387

The Three-Dimensional Evolution of a Plane Mixing Layer: Kelvin–Helmholtz Rollup

Surfaces of constant vorticity magnitude

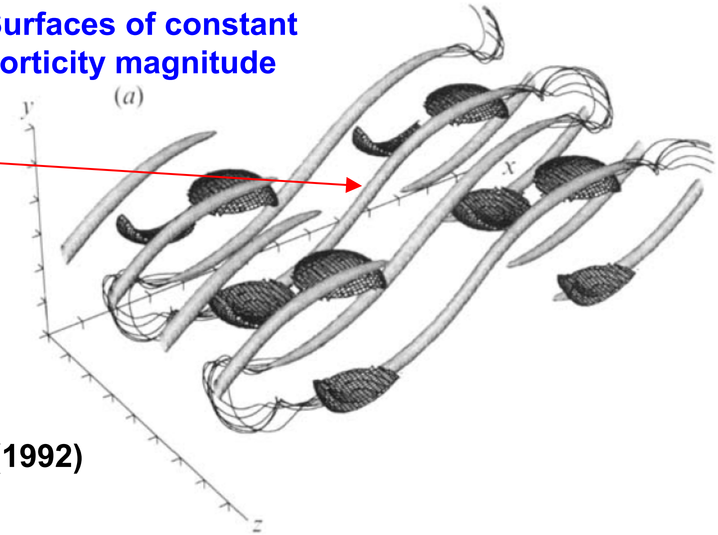

Predominantly streamwise rib vortices develop in braid region between rollers.

For certain initial conditions, persistent rib vortices do not develop. In such cases, the development of significant three-dimensionality is delayed.

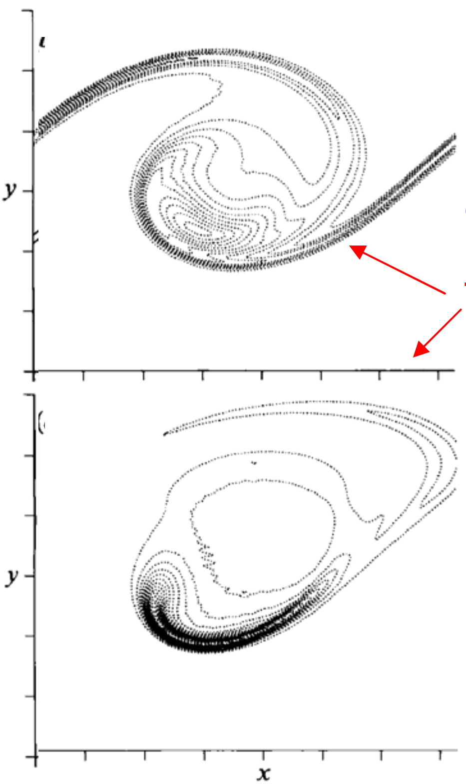

M. M. Rogers & R. D. Moser (1992)
JFM 243

Contours of ω_z indicating rollers in between ribs at two times. Solid positive. Dotted negative

vortex lines

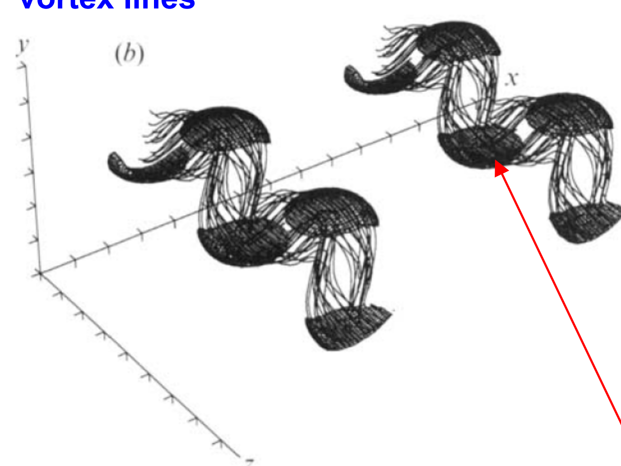

Spanwise vorticity rolls up into corrugated spanwise roller with vortex stretching creating strong spanwise vorticity in a cup-shaped region at the bends of the roller.

Spatial Relationship of Turbulent Production and Dissipation Rates to Roller Vortices in a Mixing Layer

Projection of velocity vectors on streamwise plane in a frame convecting with the mid-level velocity.

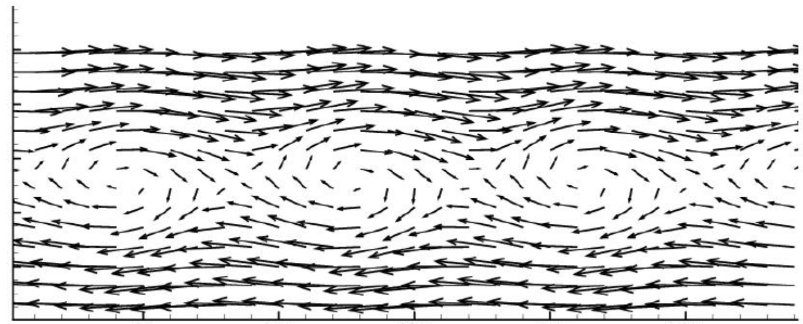

$U - U_c$

Phase averages constructed from single point measurments with 12-sensor probe and referenced to passage of roller vortices.

Reynolds shear stress (& production rate) conditionally phase averaged.

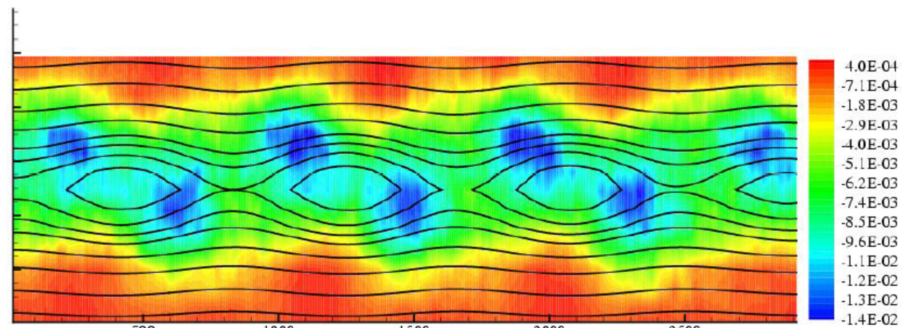

$\langle uv \rangle$

(b)

Dissipation rate conditionally phase averaged

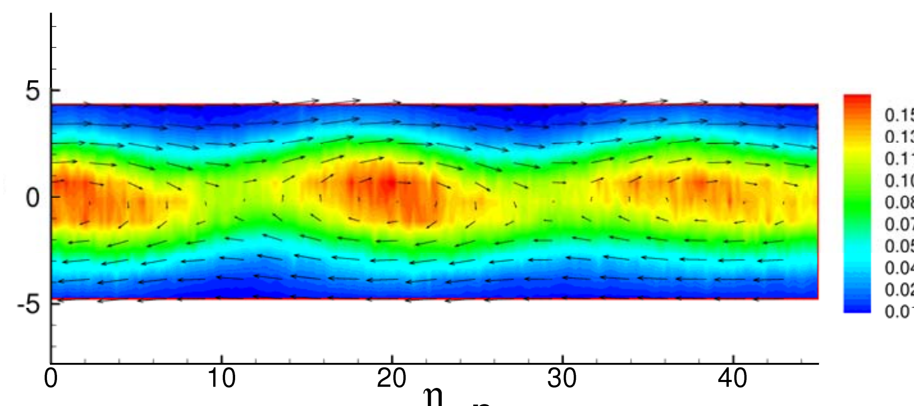

ε

η

Ph.D. Thesis, R. B. Loucks (1998)
The University of Maryland).

Animation of Turbulent Mixing Layer LES

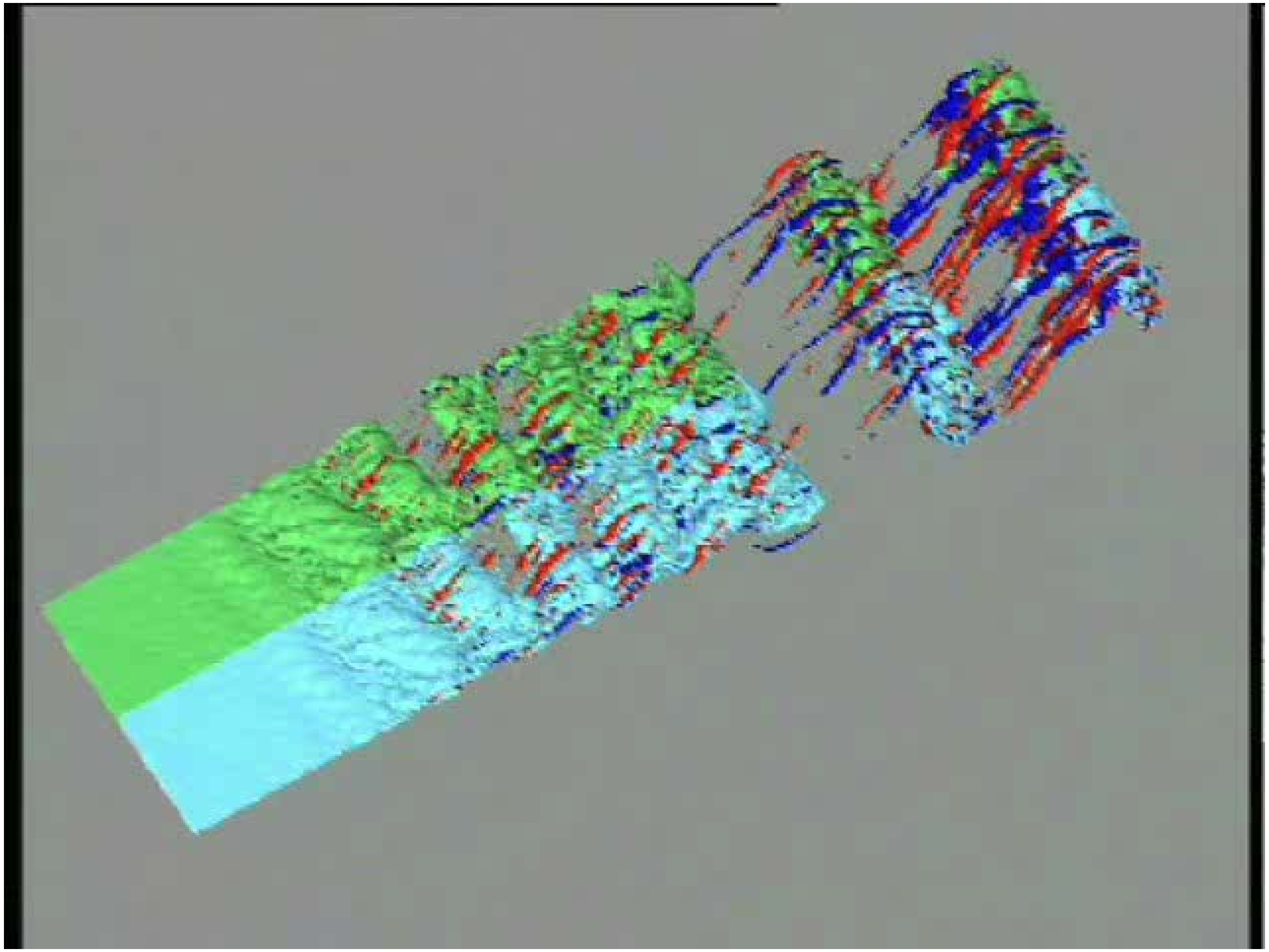

P. Comte, J. Silvestrini & P. Beégou
Eur. J. Mech B/Fluids 17 (1998)

Conclusions

Over the past twenty years remarkable progress has been made in understanding many aspects of the kinematics and dynamics of a wide variety of turbulent flows as a result of access to the velocity gradient tensor.

This progress is largely due to technological developments that have provided experimental and computational tools that were previously unavailable and to many clever people.

This great progress in understanding turbulence, in my view, shows that the oft stated idea that fluid mechanics is a "mature" field is far from true. Our best days are ahead of us!

Examples of this bright future are just up the road from me at Johns Hopkins in the PIV the theoretical/DNS work of Charles Meneveau (PRL 98, 2007) on the Lagrangian evolution of the velocity gradient tensor and the holographic PIV work of Joe Katz shown at this meeting (paper AE3).